

**Computational modeling the non-linear behavior of critical members causing progressive collapse in steel lattice towers.**

**Aiman TARIQ**



T.C.  
BURSA ULUDAĞ UNIVERSITY  
GRADUATE SCHOOL OF NATURAL AND APPLIED SCIENCES

**COMPUTATIONAL MODELING THE NON-LINEAR BEHAVIOR OF  
CRITICAL MEMBERS CAUSING PROGRESSIVE COLLAPSE IN STEEL  
LATTICE TOWERS.**

**Aiman TARIQ**  
0000-0003-0369-9091

Prof. Dr. Babür DELİKTAŞ  
(Supervisor)

MASTER OF SCIENCE THESIS  
DEPARTMENT OF CIVIL ENGINEERING

BURSA – 2020  
**All Rights Reserved**

## THESIS APPROVAL

This thesis titled “Computational Modeling the Non-Linear Behavior of Critical Members Causing Progressive Collapse in Steel Lattice Towers” and prepared by Aiman TARIQ has been accepted as an **M.Sc. THESIS** in Bursa Uludag University Graduate School of Natural and Applied Sciences, Department of Civil Engineering, following a unanimous vote of the jury below.

**Supervisor** : Prof. Dr. Babür DELİKTAŞ

**Head** : Prof. Dr. Babür DELİKTAŞ  
0000-0002-4035-4642  
Bursa Uludag University,  
Faculty of Engineering,  
Department of Civil Engineering

Signature



**Member:** Assoc. Prof. Mustafa Özgür YAYLI  
0000-0003-2333-3062  
Bursa Uludag University,  
Faculty of Engineering,  
Department of Civil Engineering

Signature




**Member:** Asst. Prof. Melih SÜRMEİ  
0000-0002-1657-1305  
Bursa Technical University,  
Faculty of Engineering and Natural Sciences,  
Department of Civil Engineering

Signature



I approve the above result



Prof. Dr. Hüseyin Aksel EREN  
Institute Director  
26..1082.020

**I declare that this thesis has been written in accordance with the following thesis writing rules of the U.U Graduate School of Natural and Applied Sciences;**

- All the information and documents in the thesis are based on academic rules,
- audio, visual and written information and results are in accordance with scientific code of ethics,
- in the case that the works of others are used, I have provided attribution in accordance with the scientific norms,
- I have included all attributed sources as references,
- I have not tampered with the data used,
- and that I do not present any part of this thesis as another thesis work at this university or any other university.

**20/08/2020**

**Aiman TARIQ**

## **ABSTRACT**

M.Sc. Thesis

**COMPUTATIONAL MODELING THE NON-LINEAR BEHAVIOR OF CRITICAL MEMBERS CAUSING PROGRESSIVE COLLAPSE IN STEEL LATTICE TOWERS**

**Aiman TARIQ**

Bursa Uludağ University  
Graduate School of Natural and Applied Sciences  
Department of Civil Engineering

**Supervisor:** Prof. Dr. Babür DELİKTAŞ

Investigations from past earthquakes have revealed that the strong seismic loads and strong wind loads can cause damage and even collapse of the steel lattice transmission towers. The effective use of all emergency equipment and infrastructure in natural disasters relies on the functioning of the electricity and communication lines. For this reason, it is very crucial to reduce the risk of damage on steel lattice towers and to maintain its functionality during and after disasters.

This thesis is aimed at investigating the collapse mechanism of steel lattice transmission tower under seismic loads and wind loads, as well as predicting the weak areas of tower. For this purpose, a systematic, accurate and reliable numerical computational model of a 55m high steel lattice tower exposed to seismic and wind loads has been created within the ABAQUS / Explicit software.

With the proposed numerical computational model, the critical elements of the steel lattice tower that triggered progressive collapse were accurately and reliably predicted. Under the highest permissible wind loads, very little damage was calculated on the leg members in the panel M of the tower, whereas under seismic loads, severe damage was calculated on all vertical leg elements in the panel M and N of the tower. It was observed that these results obtained from the numerical analysis match with collapse mechanism and weak areas formed by critical elements as a result of observation on damaged and collapsed steel towers in the field. The numerical computational model proposed in this study can be used as a guide during the design of a new tower, or it can be used to accurately predict the structural behavior and critical elements of the existing towers.

**Key words:** Lattice tower, Finite element analysis, Progressive collapse.  
**2020, ix + 68 pages.**

## ÖZET

Yüksek Lisans Tezi

ÇELİK KAFES KULELERİNDE AŞAMALI GÖÇMEYE NEDEN OLAN KRİTİK ELEMANLARIN DOĞRUSAL OLMAYAN DAVRANIŞLARININ HESAPLAMALI MODELLENMESİ.

**Aiman TARIQ**

Bursa Uludağ Üniversitesi  
Fen Bilimleri Enstitüsü  
İnşaat Mühendisliği Anabilim Dalı

**Danışman:** Prof. Dr. Babür Deliktaş

Geçmiş depremlerden yapılan araştırmalar, güçlü sismik yüklerin ve güçlü rüzgar yüklerinin, çelik kafes iletim kulelerinin hasar görmesine ve hatta çökmesine neden olabileceğini ortaya koymuştur. Doğal afetlerde tüm acil durum ekipmanların ve altyapısının etkili kullanımı, elektrik ve iletişim hatlarının işlevlerini yerine getirmesine dayanmaktadır. Bu nedenle çelik kafes kulelerinin hasar riskini azaltmak ve afet sırası ve sonrası işlevselliğini korumak çok önemlidir.

Bu tez çalışmasında, enerji nakil hatlarında kullanılan çelik kafes kulelerin, sismik yükler ve rüzgar yükleri altında çökme mekanizmasının incelenmesi ve kulelerin zayıf alanlarının tahmin edilmesi amaçlanmıştır. Bu amaç doğrultusunda, sismik ve rüzgar yüklerine maruz 55m yüksekliğindeki bir çelik kafes kule için ABAQUS/Explicit yazılımı bünyesinde, sistematik, doğru ve güvenilir bir sayısal hesaplama modeli oluşturulmuştur.

Önerilen sayısal hesaplama modeli ile çelik kafes kulelerinin, aşamalı göçmeyi tetikleyen kritik elemanları doğru ve güvenilir bir şekilde tahmin edilmiştir. Analizlerde izin verilen en yüksek rüzgar yükü altında, kulelerin M panelinde bulunan bacak elemanlarında çok az hasar hesaplanırken, sismik yükler altında ise, kulelerin M ve N panelindeki tüm dikey bacak elemanlarında ciddi bir şekilde hasar hesaplanmıştır. Sayısal analizlerden elde edilen bu sonuçların, sahada hasar görmüş ve çökmüş çelik kuleler üzerinde yapılan gözlem sonucu tespit edilen kritik elemanların oluşturduğu zayıf alanlar ve göçme mekanizması ile uyduğu görülmüştür. Bu çalışma kapsamında önerilen sayısal hesaplama modeli, yeni bir kule için sismik tasarımı sırasında bir kılavuz görevi görebileceği gibi veya mevcut kulelerin, sismik yükler ve rüzgar yükleri altında yapısal davranışını ve göçmeyi tetikleyen kritik elemanları doğru ve güvenilir bir şekilde tahmin etmek için kullanılabilir.

**Anahtar Kelimeler:** Kafes kulesi, Sonlu elemanlar analizi, Aşamalı göçme.  
**2020, ix + 68 sayfa.**

## **ACKNOWLEDGEMENT**

First of all, I would take this opportunity to thank and owe my immense gratitude to my supervisor Prof. Dr. Babür Deliktaş for accepting me as his student and for his guidance, motivation, and useful remarks throughout the course of this research. Without his expertise and insight, this thesis would not have been possible. It was a great pleasure to work with him.

During the course of this work, all the teachers at Uludag University, Civil Engineering department, my colleagues and my friends played a vital role by encouraging me to do my best and keeping my spirit up, so I would like to express my appreciation and thank all of them.

Last but not least, none of this would have been possible without the love and endless support of my family. So I would like to express my deepest gratitude to my father, mother, brother, and sister for their belief in me and constant encouragement throughout my academic endeavors.

Aiman TARIQ  
20/08/2020

## CONTENTS

	<b>Page</b>
ABSTRACT .....	i
ÖZET.....	ii
ACKNOWLEDGEMENT .....	iii
SYMBOLS and ABBREVIATIONS .....	vi
FIGURES .....	viii
TABLES.....	ix
1. INTRODUCTION .....	1
1.1 Transmission Tower.....	1
1.2 Purpose of this work .....	6
2. LITERATURE REVIEW.....	7
3. MATERIALS AND METHODS .....	12
3.1 Material .....	12
3.1.1 Type of Steel Tower and Geometric Properties .....	12
3.1.2 Geometric and material nonlinearities .....	14
3.2 Method .....	14
3.2.1 Part Module.....	15
3.2.2 Property Module .....	16
3.2.3 Step Module .....	27
3.2.4 Load Module .....	29
3.2.5 Boundary Conditions .....	34
3.2.6 Interaction Module.....	36
3.2.7 Mesh Module .....	37
3.2.8 Job Module/ Solution .....	37
3.2.9 Visualization Module/ Postprocessing.....	38
4. RESULTS AND DISCUSSION .....	39
4.1 Free Vibration Analysis and Damping.....	39
4.1.1 Free Vibration Analysis of Transmission Tower .....	39
4.1.2 Verification of Finite Element Model.....	42
4.1.3 Damping.....	42
4.2 Wind Load on Transmission Tower.....	45
4.3 Effect of increasing the wind speed on the tower .....	48
4.4 Seismic Load on Transmission Tower.....	53



4.4.1 Collapse Process of Transmission Tower .....	55
4.4.2 Behavior of Element 223 .....	57
5. CONCLUSION .....	63
REFERENCES.....	65
RESUME .....	68

## SYMBOLS and ABBREVIATIONS

Symbols	Definition
$A_e$	Effective Area of Tower
$\alpha$	Mass Proportional Damping
$a$	Acceleration
$\beta$	Stiffness Proportional Damping
$\sigma_{\text{True}}$	True Stress
$\varepsilon_{\text{True}}$	True Strain
$\sigma_{\text{eng}}$	Engineering Stress
$\epsilon_{\text{eng}}$	Engineering Strain
$\epsilon^t$	True Total Strain
$\omega_D$	State Variable
$\Delta \bar{\varepsilon}^{pl}$	Equivalent Plastic Strain
$\bar{\varepsilon}_D^{pl}(\eta, \dot{\varepsilon}^{pl})$	Plastic Strain at Onset of Damage
$\dot{\varepsilon}^{pl}$	Effective plastic strain
$\dot{u}^{pl}$	Equivalent plastic displacement at failure
$L$	Element's Characteristic Length
$U$	Displacement
$H$	Total Height of Tower
$V_b$	Basic Wind Speed
$K_0$	Conversion Factor
$K_1$	Risk Coefficient
$K_2$	Terrain Roughness Coefficient
$V_R$	Reference Wind Speed
$V_D$	Design Wind Speed
$P_d$	Design Wind Pressure
$F_w$	Wind Load acting on each panel
$kN$	Kilo Newton
$s$	Second
$m$	Meter
$G_t$	Gust Response Factor
$C_{dt}$	Drag Coefficient
$\emptyset$	Solidity Ratio
$[C]$	Damping Matrix
$[M]$	Mass Matrix
$[K]$	Stiffness Matrix
$\omega$	Natural Frequency
$\xi_i$	Critical Damping
$\Delta\omega$	Damage Index
$\nu$	Poisson's Ratio

<b>Abbreviation</b>	<b>Definition</b>
ASCE	American Society of Civil Engineers
BC	Boundary Condition
CE	Critical Elements
CAE	Computer Aided Engineering
CPU	Central Processing Unit
CDM	Central Difference Method
DUCTCRT	Ductile Damage Initiation Criterion
DEP	Dynamic Explicit Procedure
DMICRT	Damage Initiation Criterion
LTT	Lattice Transmission Tower
LA	Linear Analysis
SLT	Steel Lattice Tower
NLA	Non-linear analysis
PC	Progressive Collapse
PGA	Peak Ground Acceleration
ISE	Institution of Structural Engineers
FEM	Finite Element Method
EQL	Earthquake Load
PEEQ	Equivalent Plastic Strain
NLGEOM	Geometric Nonlinearity
RC	Rigid Connection
FVA	Free Vibration Analysis
SDEG	Scalar Stiffness Degradation
NA	Numerical Analysis
FEA	Finite Element Analysis
WL	Wind Load

## FIGURES

	<b>Page</b>
Figure 1.1. Transmission tower.....	2
Figure 1.2. Types of Lattice transmission tower structure.....	3
Figure 1.3. The collapse of transmission towers.....	5
Figure 3.1. Lattice transmission tower geometry sketched on AutoCAD.....	13
Figure 3.2. 3D Sketch of transmission tower taken from SAP2000.....	15
Figure 3.3. Elastic properties of the steel material.....	16
Figure 3.4. Elastic-plastic material behavior of steel material.....	17
Figure 3.5. Plastic properties of the material model.....	18
Figure 3.6. Stress-Strain response of a metal specimen with progressive damage.....	19
Figure 3.7. Ductile damage initiation criterions.....	21
Figure 3.8. Damage evolution criterion for the material model of transmission tower.....	22
Figure 3.9. Dog-bone specimen.....	23
Figure 3.10. Various stages of specimen accumulating plastic strain under tensile forces.....	24
Figure 3.11. Force-displacement history of the specimen.....	24
Figure 3.12. Strain vs. damage history of an element in the specimen.....	25
Figure 3.13. Stress-strain comparison between experimental results and Abaqus results.....	26
Figure 3.14. Picture representing the steps considered in seismic analysis.....	29
Figure 3.15. Wind load acting on various panels of transmission tower.....	33
Figure 3.16. El Centro N-S accelerogram.....	34
Figure 3.17. Acceleration boundary condition of transmission tower.....	35
Figure 3.18. Various jobs in Abaqus ready for simulations.....	38
Figure 4.1. Mode 1 of transmission tower.....	40
Figure 4.2. Mode 2 of transmission tower.....	41
Figure 4.3. Mode 3 of transmission tower.....	41
Figure 4.4. Displacement time history of the tower top.....	45
Figure 4.5. Members with plastic strain in transmission tower.....	46
Figure 4.6. Plastic strain time-history curve of element 119.....	47
Figure 4.7. Stress time history of element 119.....	47
Figure 4.8. Plastic strain on the various members of the transmission tower.....	50
Figure 4.9. Comparison of plastic strain values obtained from two wind load analysis.....	51
Figure 4.10. Stress time history of the element under wind loads.....	52
Figure 4.11. Stress vs. plastic strain history on element 119.....	53
Figure 4.12. Collapse mode of transmission tower.....	54
Figure 4.13. Collapse details of the lattice transmission tower under earthquake excitations.....	56
Figure 4.14. Stress time history curve of element 223.....	57
Figure 4.15. Plastic strain time history of element.....	58
Figure 4.16. Stress time history curve of element 223.....	58
Figure 4.17. Axial force-time history curve of element 223.....	59
Figure 4.18. Ductile damage time history of element.....	60
Figure 4.19. Damage time history of element.....	60
Figure 4.20. Damage initiation and failure of element 223.....	61
Figure 4.21. Similarity between the transmission tower collapse using Abaqus and real-life events.....	62

## TABLES

	<b>Page</b>
Table 3.1. Geometric properties of the lattice tower.....	13
Table 3.2. Damage initiation criterion. ....	21
Table 3.3 Transmission tower section profiles .....	27
Table 3.4. Solidity ratio and drag coefficient for various panels of transmission tower.	31
Table 3.5. Wind load acting on various panels of transmission tower. ....	32
Table 4.1. Natural frequencies belonging to notable bending and twisting modes of the transmission tower. ....	39
Table 4.2. Comparison of frequencies between two programs. ....	42
Table 4.3. First two natural frequencies of transmission tower. ....	44
Table 4.4. New calculated wind loads after increasing the wind speed.....	49

# **1. INTRODUCTION**

## **1.1 Transmission Tower**

In the current generation, no one can imagine a world without electricity as it plays a pivotal role in the economic development of any country. Electricity has dominated major areas of our lives, thus becoming one of the most important necessity for our survival. Electricity is being consumed for using every electrical and electronic device and machines in everyday life. Without the availability of electric power, the whole world would standstill. There are many places which need electricity, but the generation of electricity is not possible there due to lack of resources or due to the location of those places being very far away from populated areas. Therefore, in those cases, power transmission systems play a crucial role in transporting power from power generating stations to those places.

Steel lattice towers that are widely used as supporting structures in various civil engineering works such as radio and television broadcasting are used for electric transmission as well (Figure 1.1). Some steel towers have been in operation for almost a century. The best example of steel lattice towers is the Eiffel tower, which is both architectural and engineering marvel.

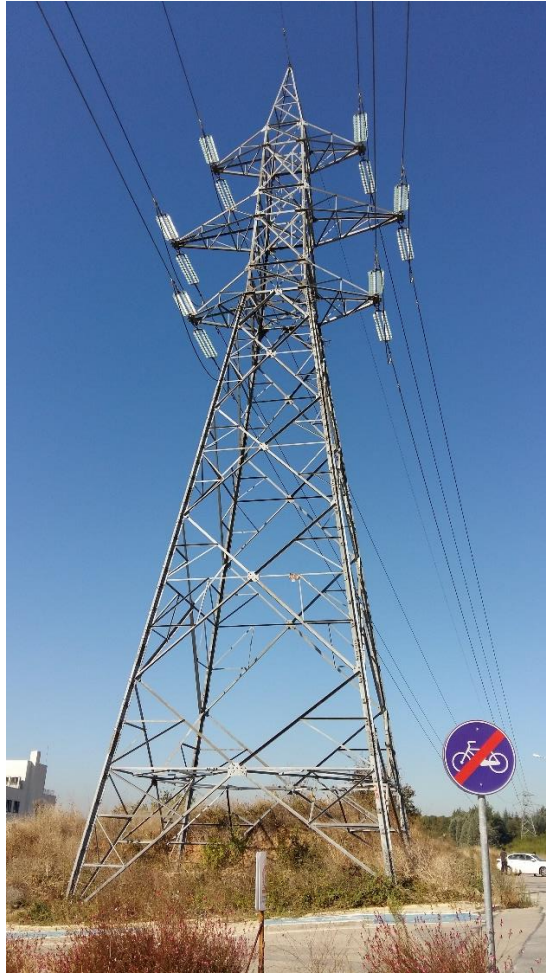


**Figure 1.1.** Transmission tower (picture of transmission tower nearby metro station at Özlüce)

Lattice towers are graded in two main categories, such as guyed towers and self-supporting towers. The main focus of this study is on self-supporting towers, also called transmission towers, which are used in the transmission of high voltage conducting wires. These transmission towers have excellent structural stability which makes them perfect for safe and reliable electric power distribution from stations to remote areas (Siddam 2014).

The height of these transmission towers can range from 30-50 meters placed at an interval of 200-600 meters. These towers are reasonably lightweight in comparison to other traditional structures. One of their noticeable property is that they are greatly efficient in

respect of load-carrying capacity to weight ratio. Furthermore, its manufacture and assembly is quite easy and fast.

A transmission tower is made up of main legs, horizontal and vertical bracings. Its members are typically composed of  $90^\circ$  angle sections or sometimes round tubular sections. There are many configuration designs of transmission tower available but, depending on the parameters such as the amount of transmitted power, the topography of area (mountain, river, cities), and environmental factors (wind, temperature), the appropriate configuration is chosen. Some transmission tower configurations based on voltage carrying level are shown in Figure 1.2.

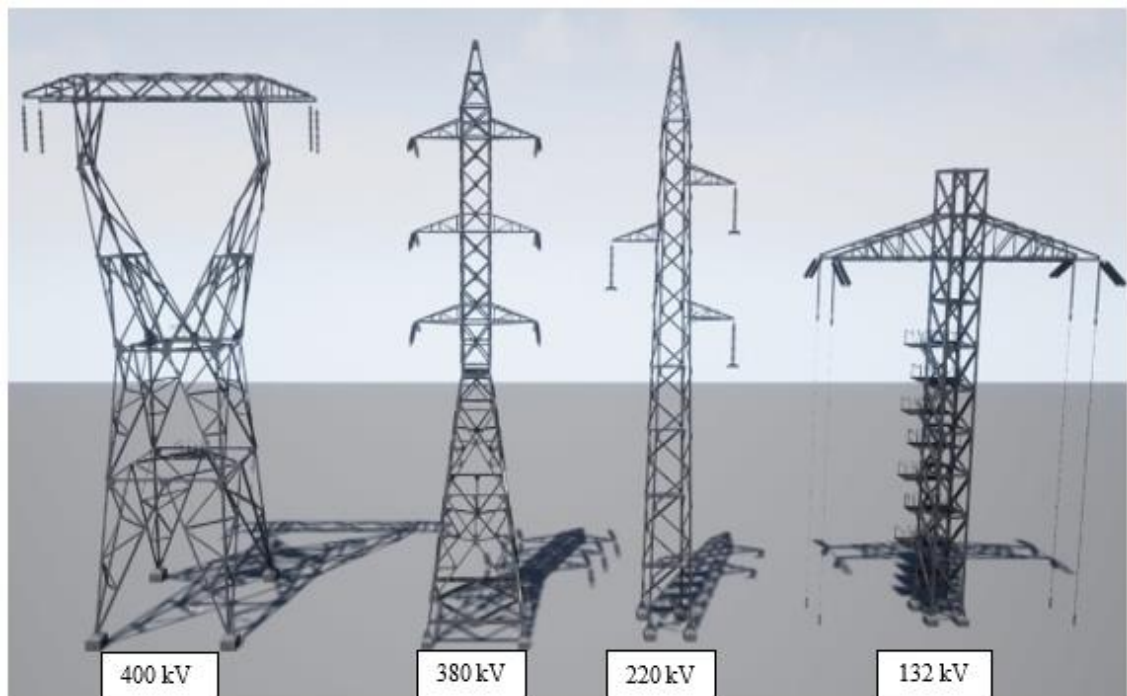


**Figure 1.2.** Types of Lattice transmission tower structure. (Gooseman, 2020)

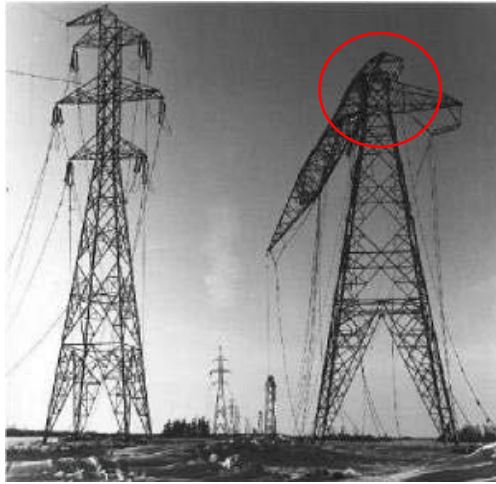
It is very important to have detailed knowledge of structural behavior of transmission towers to design, construct, and maintain these structures more efficiently, economically, and safely. Keeping those points in view, the structural analysis of transmission towers has turned out to be one of the most important areas of research. In current times there are many computer-aided software based on finite element method present which are able to conduct linear and non-linear analysis of lattice towers (Ahmed, 2007).



A large part of design load on the transmission tower constitutes dead weight which includes self-weight of tower and weight of heavy wire loadings that carry electricity. These transmission towers are designed to resist wind load without taking earthquake load into consideration. However, sometimes these towers may be located in high-risk seismic areas, or sometimes the owner desires them to survive a strong earthquake. One such example of this was seen in Taiwan (1999) when the Chi-Chi earthquake occurred, which caused extensive damage to the electric power system resulting in the collapse of 15 transmission towers, 26 towers damaged, and 69 transmission lines destroyed. This earthquake caused complete blackout because of no electricity, and also wired and wireless telecommunication was disrupted for the next 36 hours in central and northern regions of Taiwan (Loh and Tsay, 2011). Again, in China (2008) lot of damage took place under Wenchuan earthquake, which left 20 lattice towers of 110kV collapsed to the ground and one 220kV transmission line destroyed very badly in Mao County.

Transmission towers are repeatedly exposed to severe environmental conditions such as high-intensity winds, earthquakes, downbursts. As a consequence of those extreme conditions, the tower could lose some of their critical structural members due to loss of load-bearing capacity, followed by the collapse of a structure partially or fully. This phenomenon is called a progressive collapse. According to the American Society of Civil Engineers (2013), progressive collapse can be defined as the growth of initial local failure starting from an element then spreading to other elements, finally resulting in the collapse of the whole structure or significant part of it. At the same time, The Institution of Structural Engineers (2013) compared the progressive collapse of a structure to collapse of a row of dominos, which takes place in a progressive manner. Cuoco (1997) stated that when the progressive collapse takes place, the member damage affects a tiny part of a structure at the start, then it is likely to propagate to further parts of the structure as well and may eventually result in collapse of the whole structure. This sort of failure mechanism has been coined as a progressive collapse. Therefore, briefly progressive collapse is an event in which structure collapses consistently owing to local damage and

loss of structural members. The activation of progressive collapse in transmission tower is usually triggered by the sudden loss of one or more critical elements (Figure 1.3).



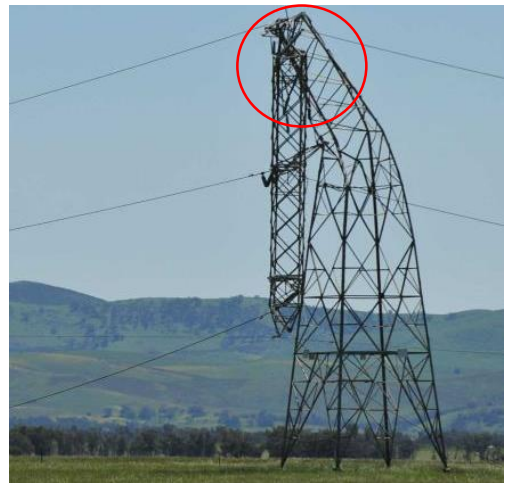
a) (Siddam, 2014)



b) (Wurst, 2017)



c) (Shehata, 2020)



d) (Faulkner, 2016)

**Figure 1.3.** The collapse of transmission towers.

As shown in Figure 1.3 (a), (b), (c), (d), a common failure pattern can be observed in these pictures. The region where the damage took place in all of these transmission towers is same. The collapse of transmission towers has occurred due to the damage that took place in the members present in the top portion of tower just near the region where the

cross arms carrying the electric conductors and body of tower meet. The collapse of different transmission towers shown in the pictures above has mostly occurred under ice storm or wind storm in different parts of the world. Hence it can be said that the area encircled in the photographs is the weak area and is very susceptible to damages.

Therefore, an analysis called as progressive collapse analysis is done for simulating the progressive collapse events with the purpose of evaluating collapse mode, vulnerable areas, and capacity of structure. The result from this analysis can be useful for evaluating existing structures or for the design of new structures.

## **1.2 Purpose of this work**

The purposes of this work are-

- to determine the mechanical behavior of the critical elements that lead to the progressive collapse of the steel transmission tower by developing a computational model within the scope of the finite elements.
- to investigate the damages caused due to wind load and seismic load on the critical elements of the transmission tower by performing non-linear finite element analysis using developed computational model within ABAQUS/Explicit.
- to determine the effects on the tower by increasing the wind loads to maximum permissible by the codes.
- to capture the final failure mode of the transmission tower and subsequently, predict the weak area of the tower that eventually causes progressive collapse of the tower.

## 2. LITERATURE REVIEW

In this chapter, the literature review of the relevant publications on damage in transmission towers due to dynamic wind and earthquake is summarized. There have been numerous experimentally and numerically studies performed on the dynamic behavior of the transmission towers.

Wang et al. (2012) performed a progressive collapse analysis of transmission tower under various earthquake excitations along longitudinal and lateral direction based on finite element method (FEM) program ABAQUS. Analysis was performed to study the effect of ultimate strain on collapse mode and capacity. While conducting the numerical simulation, they retained the element mass rather than removal after they lose load-bearing capacity. It was found from the analysis results that the main leg member of tower at the height of 34.9m from ground was more vulnerable to yield and to lose bearing capacity than any other member. They observed that there was an exceptional increase in the collapse resistance of tower with an increase in the ultimate strain and concluded that collapse resistance can be improved by strengthening the weak locations. Finally, they suggested using three or more ground motion time history for conducting collapse analysis of transmission tower.

Eslamlou and Asgarian (2017) presented a paper for determining the critical members of 400kV electric transmission tower subjected to progressive collapse by using OpenSees program for numerical modelling and performing non-linear dynamic analysis of tower. They used impact factor and capacity to demand ratio method for checking critical areas of a transmission tower and were successful in predicting the key members responsible for causing the progressive collapse. The structural members having maximum impact factor and minimum capacity to demand ratio were found to be most crucial members. They also found from results that maximum impact factor was in the lower height of tower legs which means that tower legs with lower elevation are more susceptible to start progressive collapse. For verification of the analysis results, authors took the structural

model from the article by Prasad Rao et al. in which NE- NASTRAN program was used. The results between OpenSees and NE- NASTRAN were seen to be in close agreement with each other.

An et al. (2018) conducted a research on the collapse of 13 electric transmission towers in the Hainan region of China due to extreme typhoons. They carried out a failure analysis of towers considering both wind load as well as heavy rain load using finite element analysis model on ANSYS program. They used linear 2-node beam element in 3-D suitable for modelling tower leg members. The simulation results showed that failure mode and failure areas of structure were in good agreement with the post-event field observation. Buckling was observed in the main leg member of the tower due to presence of extremely high stress, which was leading to the collapse of transmission tower. They suggested that higher values of wind parameters  $\alpha_w$ ,  $\beta_z$ ,  $\beta_c$  should be used while designing a transmission tower to counter severe environmental conditions in coastal areas.

Tian et al. (2018) conducted a full scale experiment as well as numerical simulations on electric transmission towers to study its failure mechanism. The structure was subjected to different types of loading patterns such as broken wire, wind load, and ice load to investigate its load-bearing capacity. They used ABAQUAS, which is a numerical simulation program to make a detailed finite element model of tower structure for failure process using an explicit method and then later compared its results with the result from full-scale tests. They modelled the structural members with beam element (B31) in ABAQUS with rigid connection and fixed its base nodes to ground. They observed that ultimate-load bearing capacity and failure mode of structure acquired from full-scale experiments are very identical to numerical simulations and also found that members near cross arms were very vulnerable to fail. Since the good agreement was found between the numerical method and full-scale experiment, the authors recommended that the proposed numerical method for finite element model is very effectual and reasonable way of conducting failure analysis of a structure.

Rao et al. (2010) conducted full-scale tests on 5 transmission towers of different configurations to find the failures and its reason in detail. They modelled all the angle members of structure using beam-column elements. Non-linear finite element analysis software NE- NASTRAN was used for modelling then a comparison between experimental full-scale test results with numerical results was made. Testing was conducted under Indian standard code specifications such that the load is applied in the increments and at each increment load was retained for a minimum of two minutes. They observed various types of failures in the towers at different locations such as failure in leg members and bracing members, which took place below the waist level of every tower. In some areas, failure was caused due to insufficient capacity in the redundant member. It was clearly visible from results that large member forces in structural elements could be acquired from non-linear analysis, as compared to linear static analysis.

Zhang et al. (2013) presented a paper in which they conducted the progressive collapse of an electric transmission tower and tower line system caused by strong winds in order to focus on its dynamic behaviour and mechanism. They created a finite element model of tower and tower line system in numerical simulation program ABAQUS/Explicit for the progressive collapse simulation works. They fixed the base nodes of the tower to ground and assigned the members of the tower as B31 beam elements and earth wires as T3D2 truss elements. They found from the analysis results that collapse pattern of tower depends on the position, number, and deformation of damaged elements, and progressive collapse path is influenced by conductors and wires. They recommended that due to the presence of ground wires and conductors in transmission tower-line system, highly accurate results can be achieved from for progressive collapse simulation rather than a single tower with the same loading conditions and method.

Eltaly et al. (2014) conducted research that focussed on predicting the failure mechanism of transmission towers using non-linear finite element models in ANSYS software by including the material and geometrical nonlinearity. In this research, the author used L section beam elements for the tower members and took eccentricity and joint effect of the structure into consideration. The results demonstrated that the FE model with joint

slippage and eccentricity in its members is in good agreement with the experimental test results. They concluded that the type of connection in the lattice tower can change the ultimate behaviour of structure but does not affect the failure mode of the tower.

Tian et al. (2013) performed a progressive collapse analysis of 500kV electric transmission tower subjected to earthquake excitations using a non-linear time history method. The 3D finite element model of transmission tower was made in the ABAQUS program for carrying out the simulation using 3 seismic records, and three-dimensional B31 beam elements were assigned to structural members. They were successfully able to observe failure position and collapse routine of the tower through simulation. They recommended that at least three seismic waves should be used for failure analysis because collapse paths and fracture positions are different for every seismic wave. They also advised that the result obtained from the simulation can be utilised for designing and reinforcement of transmission tower.

Fu et al. (2019) conducted thorough tests of transmission towers under the strong wind loads and broken line conditions to inspect their strength capacities and failure mechanism. The full scale test was executed by subjecting the tower to eight different loading patterns. The author also conducted uncertainty analysis to discover the potential failure positions in the tower. They found from the full scale tests that the first failure position started in the leg member of the tower, and when the applied load is reduced to zero, the remaining strain on the member is more than the initial stain. They concluded that the failure positions that were forecasted with the help of uncertainty analysis are in good agreement with the experimental test results.

From all the literature review done that has been done in this chapter, a few shortcomings, especially in modelling aspect, can be observed. No work in the given literature has provided a detailed explanation of the material model, which is very crucial for performing the progressive collapse. As well as most studies are just focussed on determining the failure positions and weak areas of the tower without giving much attention towards studying the non-linear behaviour of critical elements. Therefore, there

is a need for a study that will cover these shortcomings and propose a non-linear dynamic technique that will provide reliable results. Hence the work done in this thesis will remove these shortcomings and will also provide the systematic numerical modelling steps and details that is believed to contribute to the field.



### **3. MATERIALS AND METHODS**

As mentioned in the chapter 1 the aim of this study is to predict the mechanical behavior of critical members causing progressive collapse in steel transmission tower under wind and seismic loads by developing a computational model within the framework of ABAQUS/Explicit finite element program. This section provides a brief overview of the Abaqus program and structural models used in this study. Taking geometry and material non-linearity into consideration, the method used for analyzing the structural model has been discussed as well.

#### **3.1 Material**

This unit describes the details about materials, geometric properties, various loads acting on the tower, type of steel tower, and geometric and material non-linearity that have been used in this work.

##### **3.1.1 Type of Steel Tower and Geometric Properties**

Commonly steel or aluminum are used for constructing lattice towers. Aluminum is used at critical places for reducing weights, such as while positioning the tower in the mountainous areas using the helicopter. Aluminum is also preferred in the steel corrosive environments. As far as steel towers are concerned which are stronger in nature, they can be used to make very tall towers up to the height of 100m possible. In this work, a 240 kV double circuit, self-supporting steel lattice transmission tower with a square base having K type bracing in the bottom part and X type bracing in the middle and top part has been used. This type of structure is widely used around the world because of being economical, its ability to carry high voltage and resist forces resulting from wind loads, conductor and ice loads. The lattice tower with a height of 55m and a base width of 12.5 × 12.5 m has been used in this work. This lattice tower consists of 5 sections, which are 4 cross arms, a cage (the top vertical portion of the tower surrounded by cross arms), a tower body (bottom portion of the tower below the cross arms), and 4 legs.

**Table 3.1.** Geometric properties of the lattice tower.

Section	Length (m)
Cross arm	5.40
Cage	15.3
Tower body	32.5
Legs	7.5
Base width	12.5
Top width	2.20
Total height	54.8

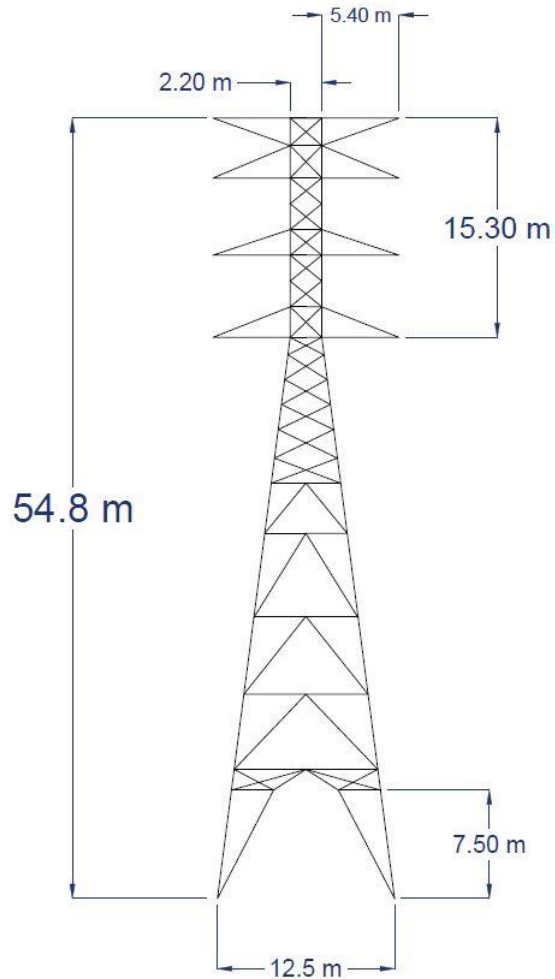


**Figure 3.1.** Lattice transmission tower geometry sketched on AutoCAD.

### **3.1.2 Geometric and material nonlinearities**

In this work, geometric nonlinearity of the model is taken into consideration because the structure is expected to experience large deformations in order to maintain its equilibrium under high loads. Large deflections in the tower change the shape of the structure, and hence its stiffness matrix changes. In addition to that, material nonlinearity is considered as well because steel has a linear stress/strain relationship at small strain values. However, when the strain values become large, the material starts to yield and demonstrates non-linear response which is irreversible. So an elasto-plastic steel material model which includes the material nonlinearity has been used in this study. A non-linear analysis is preferred because it produces a realistic representation of progressive collapse events. Results obtained from these non-linear analysis gives a clearer structural response, provide more accurate results as well as provides an excellent opportunity for the evaluation of progressive collapse of structures.

### **3.2 Method**

In this section, systematic detailed procedures for establishing the computational model within ABAQUS is presented. Abaqus is a finite element analysis simulation software for solving engineering problems, which include linear and non-linear structural analysis, static, dynamic and heat transfer analysis.

Abaqus provides a simple interface for creating, submitting, monitoring, and evaluating results from simulations. Abaqus has different modules where each module defines a logical aspect of the modeling process, for example Part Module allows one to perform the all the sketches of parts for the structural model, Property Module where materials model and sections are defined, Step Module where type of the solver, increment size, controlling and output variables are chosen, Interaction Module, where all the interaction and contact among parts of the structure are defined, Load Module where all the applied loads and boundary condition are defined, Mesh Module where type of element and meshing size are defined, Job Module creates job for analysis and final Visualization

Module that allows one to view the results of the analysis and perform the post processing on the results.

### 3.2.1 Part Module

The geometry of the transmission tower structure is very complex therefore, constructing its three-dimensional model, which consists of hundreds of members in the Abaqus program is very time consuming and complicated. It is more effective to sketch a 3D model of a tower in second party software and then export it to Abaqus. Therefore, in this thesis, a complete model of transmission tower as shown in Figure 3.1, was established in SAP2000 and then was saved as IGES file. The saved IGES file was imported in Abaqus part module as a 3D deformable geometry. After importing the geometry from SAP2000 no further changes or additions were made in the model geometry.

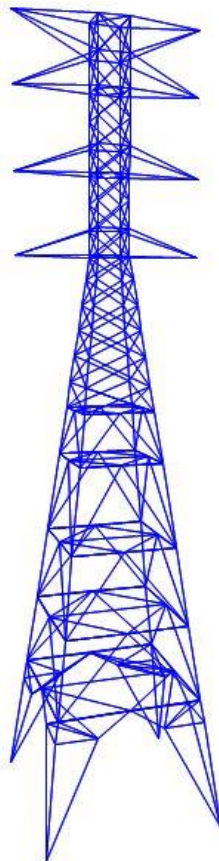


**Figure 3.2.** 3D Sketch of transmission tower taken from SAP2000.

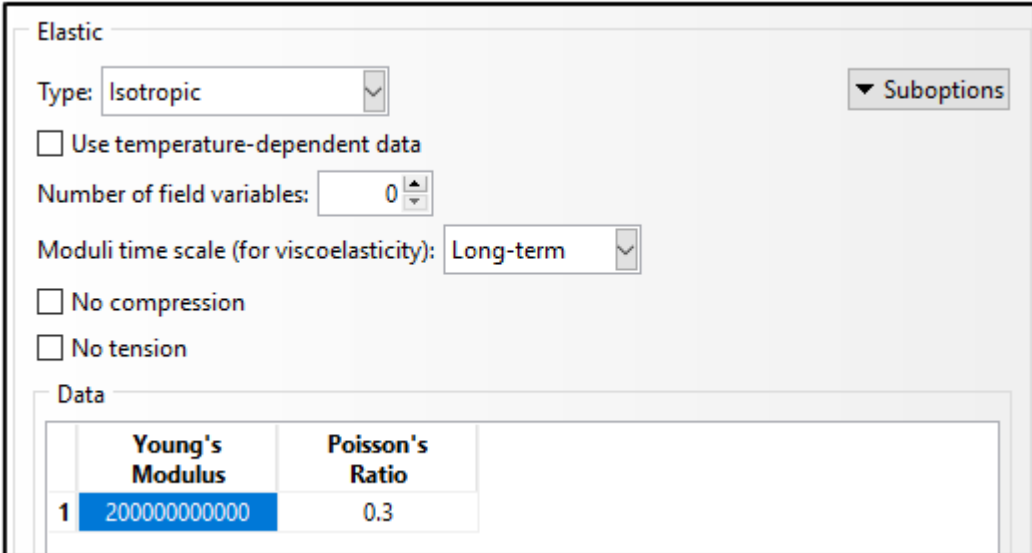
### 3.2.2 Property Module

#### 3.2.2.1 Material Model

In this work, steel material has been used in all the members of transmission tower with the uniform mass density of  $7800 \text{ kg/m}^3$ . Material properties were modeled with elastic-plastic behavior incorporating non-linearity to acquire the effects of plasticity, progressive damage and failure.

##### 3.2.2.1.1 Elasticity

An isotropic type elasticity has been selected for this analysis because it is the simplest method for describing linear elasticity. In isotropic type, elastic properties are specified by providing the values for Young's modulus and Poisson's ratio. Hence, the material elasticity used in this model was defined with \*ELASTIC option in Abaqus by inputting Young's modulus as 210 GPa and Poisson's ratio as 0.3.



The image shows a software interface for defining elastic properties. The 'Elastic' section is active, with 'Type' set to 'Isotropic'. There are several checkboxes: 'Use temperature-dependent data' (unchecked), 'No compression' (unchecked), and 'No tension' (unchecked). The 'Number of field variables' is set to 0, and the 'Moduli time scale (for viscoelasticity)' is set to 'Long-term'. Below these options is a 'Data' table with two columns: 'Young's Modulus' and 'Poisson's Ratio'. The first row of data shows a Young's Modulus of 200000000000 and a Poisson's Ratio of 0.3.

	Young's Modulus	Poisson's Ratio
1	200000000000	0.3

**Figure 3.3.** Elastic properties of the steel material.

### 3.2.2.1.2 Plasticity

The plasticity for this material model was defined using the \*PLASTIC option in Abaqus. The stress-strain curve belonging to the tensile test performed on a specimen is given in Figure 3.4 below. This data was later processed and inputted in Abaqus as a true stress-plastic strain form for defining plasticity.

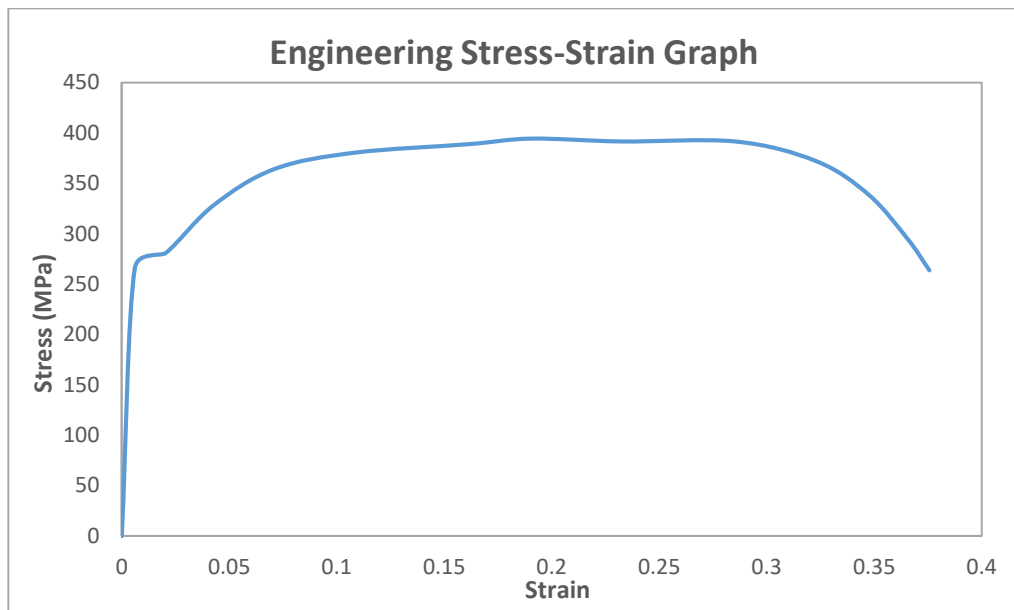


**Figure 3.4.** Elastic-plastic material behavior of steel material. (Pavlović, 2013)

Abaqus requires true stress and plastic strain for defining the plasticity, whereas the stress-strain values obtained from the tensile test data are engineering stress-strain values. Therefore, the relationship to convert from engineering stress to true stress is given as:

$$\sigma_{True} = \sigma_{eng}(1 + \varepsilon_{eng}) \quad (3.1)$$

and to convert from engineering strain to true strain is given as:

$$\varepsilon_{True} = \ln(1 + \varepsilon_{eng}) \quad (3.2)$$

The plastic strain values that are given to Abaqus while defining plasticity is calculated from the relationship written as:

$$\varepsilon^{pl} = \varepsilon^t - \frac{\sigma_{true}}{E} \quad (3.3)$$

Where  $\varepsilon^t$  is true total strain,  $\sigma_{true}$  is true stress, and  $E$  is Young's modulus.

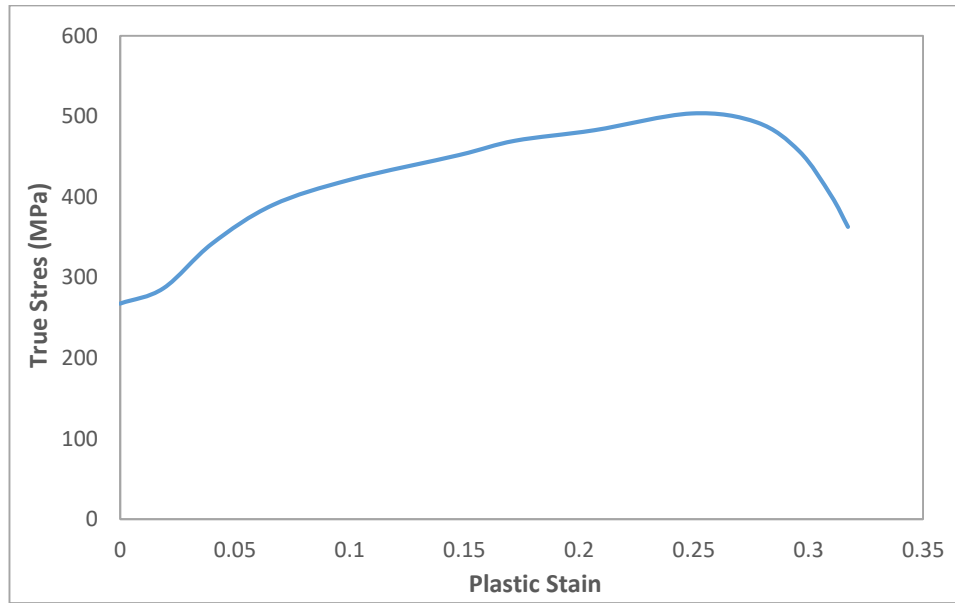


**Figure 3.5.** Plastic properties of the material model.

### 3.2.2.1.3 Progressive Damage and Failure Model

In order to capture progressive damage of the structure due to material failure in ductile metals, a ductile damage material model that describes the stiffness degradation is summarized here.

A stress-strain response of a simple tensile test of any metal specimen is shown below to demonstrate progressive failure modeling in Abaqus.

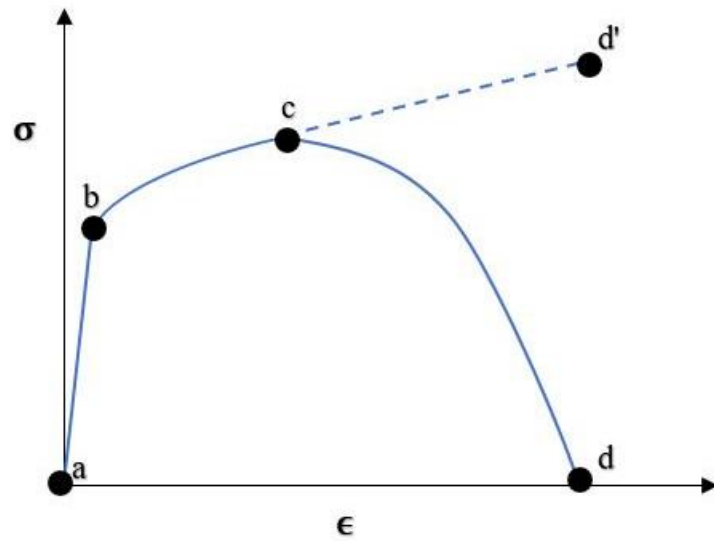


**Figure 3.6.** Stress-Strain response of a metal specimen with progressive damage.

As shown in the figure above, various phases of stress-strain response can be noticed. In the first phase  $a - b$ , the response shown by ductile material is linear elastic at the start, which is led by  $b - c$  where plastic yielding and strain hardening in the material can be observed. A notable declination in the load-carrying capacity of the specimen is visible after  $c$  until the point of rupture at  $d$ . The deformation in the  $c - d$  phase takes place in the specimen's neck region. Point  $c$  is defined as damage initiation criterion. After point  $c$ , the specimen's response  $c - d$  is controlled by degradation of stiffness in the area of strain localization. The response curve  $c - d$  is just the degraded response of curve  $c - d'$  that material would have shown in case of damage.

Thus, the failure mechanism of metal has three noticeable parts:

1. Undamaged material response ( $a-b-c-d'$ )
2. Damage initiation criterion ( $c$ )
3. Damage evolution ( $c-d$ )

### 3.2.2.1.3.1 Damage Initiation Criterion

Material's damage initiation feature in Abaqus has the potential to predict the initiation of damage in metals and other materials. Since just the steel material has been used in this work so the main focus will be on steel only. The mechanism due to which the fracture



in steel material occurs is the ductile fracture, and the reason for this ductile fracture is initiation, growth, and coalescence of micro-cracks/voids under various loads. The purpose of defining the ductile criterion is to predict the onset of damage on a member by assigning the equivalent plastic strain, stress triaxiality and strain rate. The damage initiation process starts the moment when the following equation is met:

$$\omega_D = \int \frac{d\bar{\varepsilon}^{pl}}{\varepsilon_D^{pl}(\eta, \dot{\varepsilon}^{pl})} = 1 \quad (3.4)$$

$\omega_D$  in this equation represents the state variable that grows uniformly along with plastic deformation of a member. Calculation of the incremental growth of state variable  $\omega_D$  at any increment in the course of analysis can be done with the following equation:

$$\Delta\omega_D = \frac{\Delta\bar{\varepsilon}^{pl}}{\varepsilon_D^{pl}(\eta, \dot{\varepsilon}^{pl})} \geq 0 \quad (3.5)$$

Here,

$\Delta\bar{\varepsilon}^{pl}$  = Equivalent plastic strain value at the particular increment, which is calculated in Abaqus and it can be displayed in the visualization module under PEEQ option.

$\bar{\varepsilon}_D^{pl}(\eta, \dot{\varepsilon}^{pl})$  = Plastic strain at the onset of damage which depends on stress triaxiality and strain rate.

This value is defined by the user while inputting the damage initiation properties in the material's ductile damage. Ductile damage initiation criterion  $\omega_D$  can be used to check if ductile damage process has been started or not at any increment in Abaqus visualization module under DUCTCRT option (Abaqus, 2014)

Therefore, in this thesis, the damage initiation criterion for steel material to be used for transmission tower is given in Table 3.1 below:

**Table 3.2.** Damage initiation criterion.

Fracture Strain ( $\bar{\epsilon}_D^{pl}$ )	Stress Triaxiality ( $\eta$ )
0.0948	0.92

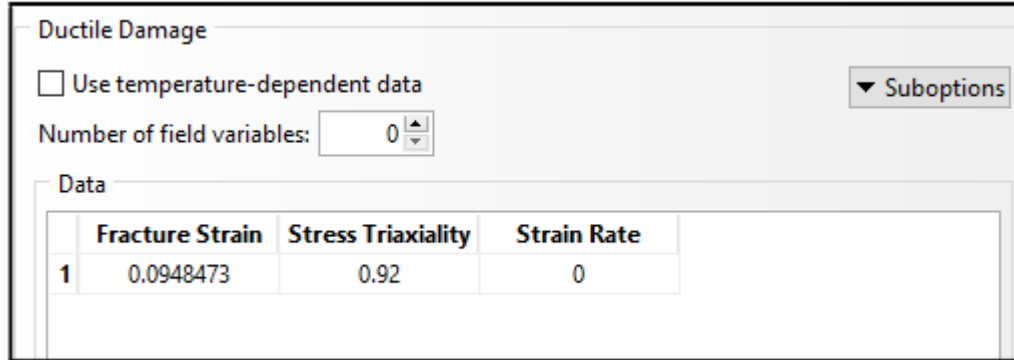


**Figure 3.7.** Ductile damage initiation criterions.

### 3.2.2.1.3.2 Damage Evolution

The rate by which the degradation of material stiffness occurs after the damage has been started in a ductile metal is given by damage evolution law. This law decides the response of material after damage initiation. When the damage variable  $D$  reaches the value 1, material fails completely and fracture occurs as well (Abaqus 2014). Generally, there are two ways by which damage evolution can be defined in Abaqus

1. In terms of equivalent plastic displacement
2. In terms of fracture energy

In this work, damage evolution was defined in terms of equivalent plastic displacement. Equivalent plastic displacement at failure has been determined based on the equation below:

$$\dot{u}^{pl} = L \dot{\epsilon}^{pl} \quad (3.6)$$

Where,

$L$  = Element's characteristic length, which is equal to the mesh size used in the model.

$\dot{\bar{\epsilon}}^{pl}$  = Effective plastic strain, which is equal to plastic strain accumulated during the damage process, i.e. the difference between plastic strain at fracture  $\bar{\epsilon}_f^{pl}$  and at the onset of damage  $\bar{\epsilon}_D^{pl}$ . Therefore,  $\bar{\epsilon}_f^{pl} = 0.175$  obtained from the yield stress-plastic strain values that are inputted while defining plasticity in the Abaqus, and  $\bar{\epsilon}_D^{pl} = 0.0948$  obtained from Table 3.1. Hence, effective plastic strain  $\dot{\bar{\epsilon}}^{pl} = 0.175 - 0.09484 = 0.080$ .

Every element in this model is assigned with a mesh of 1 unit, and it has been multiplied with the effective plastic strain of 0.080 to get equivalent plastic displacement at failure.

Therefore,

$$\dot{u}^{pl} = 1 * 0.080$$

$$\dot{u}^{pl} = 0.08015$$

Damage evolution is assigned in Abaqus under the sub-option button inside ductile damage module.

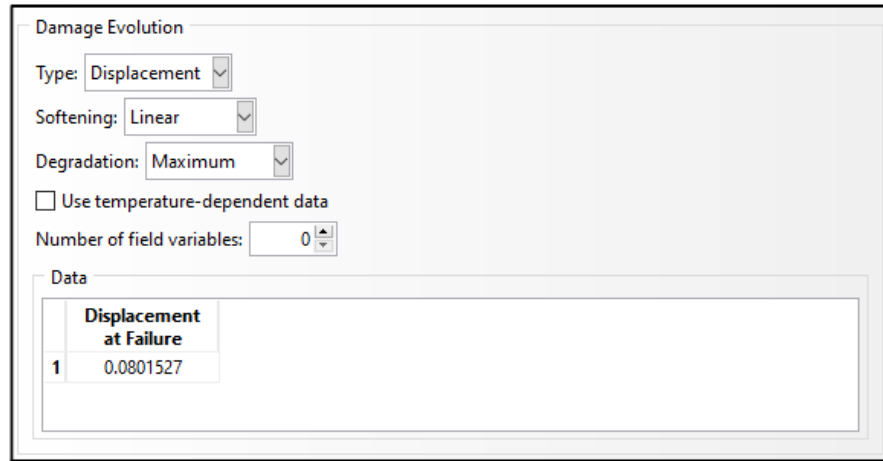


**Figure 3.8.** Damage evolution criterion for the material model of transmission tower.

### Uniaxial Tensile Test on a Steel Dog-bone Specimen

With the aim of verifying the material model that has been used in this thesis, especially the plasticity and ductile damage, a uniaxial tension test has been conducted on a steel dog-bone specimen in Abaqus environment. The geometry of the dog-bone specimen having a thickness of 5mm is given in Figure 4.4 below.

The damage initiation criterion of this specimen will be different as that of transmission tower because of the different shape, size, and type of element used in this analysis. The damage initiation criterion is set as 0.34 and damage evolution as 0.316.

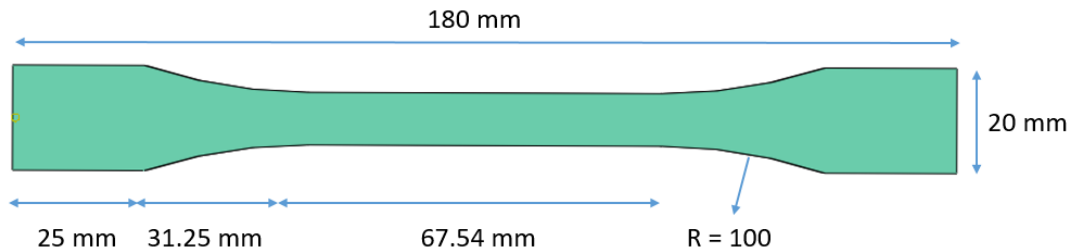


**Figure 3.9.** Dog-bone specimen.

The specimen shown above was modeled in Abaqus program, and then it was assigned with the material properties as explained in the unit 3.2.2.1 of this thesis. One end of this specimen has been held fixed in all directions. In contrast, the other end was held fixed in only U1 and U3 direction, allowing U2 to have a displacement of 30 mm in the opposite longitudinal direction in order to create the tension forces in the specimen. The analysis was conducted with a dynamic explicit method and was processed for the duration of 1 second.

The analysis was completed successfully, and the results showed the splitting of the specimen into two parts as a result of ductile damage on it. The specimen behaved exactly the same way as it was expected from it. The various stages of the specimen having plastic strain (PEEQ) accumulated on its body are shown in Figure 3.10. The force-displacement pertaining to the specimen is also given in Figure 3.11. The maximum force that the specimen could take was calculated as 18.6 kN. Once the specimen reaches its maximum load taking capacity, it gets damaged and subsequently splits into two pieces. The noticeable downfall in Figure 3.11 represents the splitting of the specimen. After this event, the specimen cannot bear any more loads.

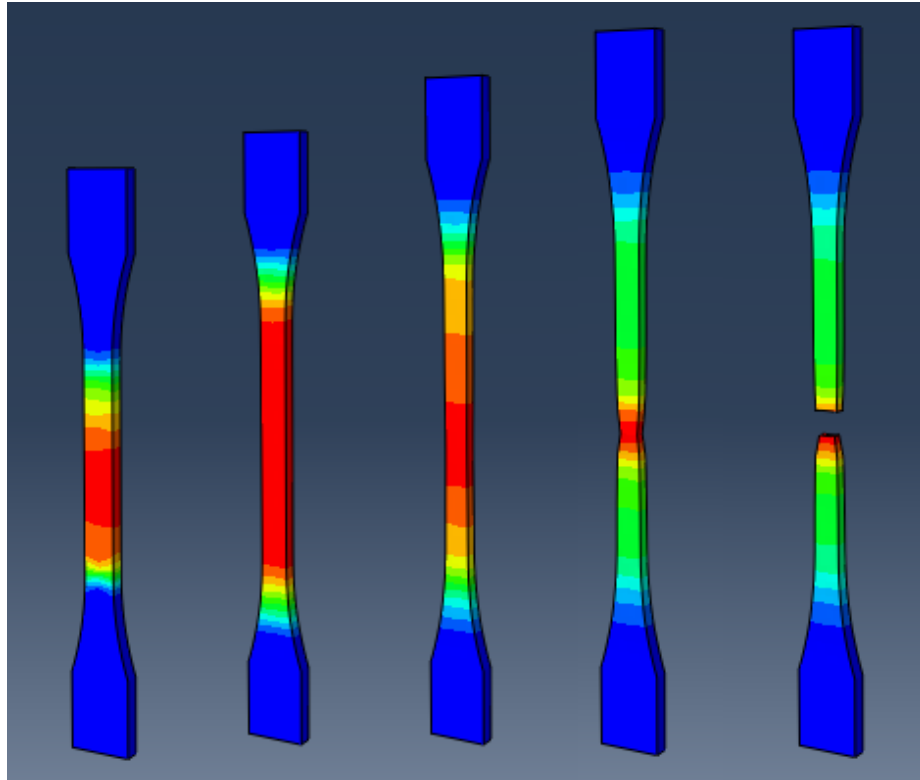


**Figure 3.10.** Various stages of specimen accumulating plastic strain under tensile forces.

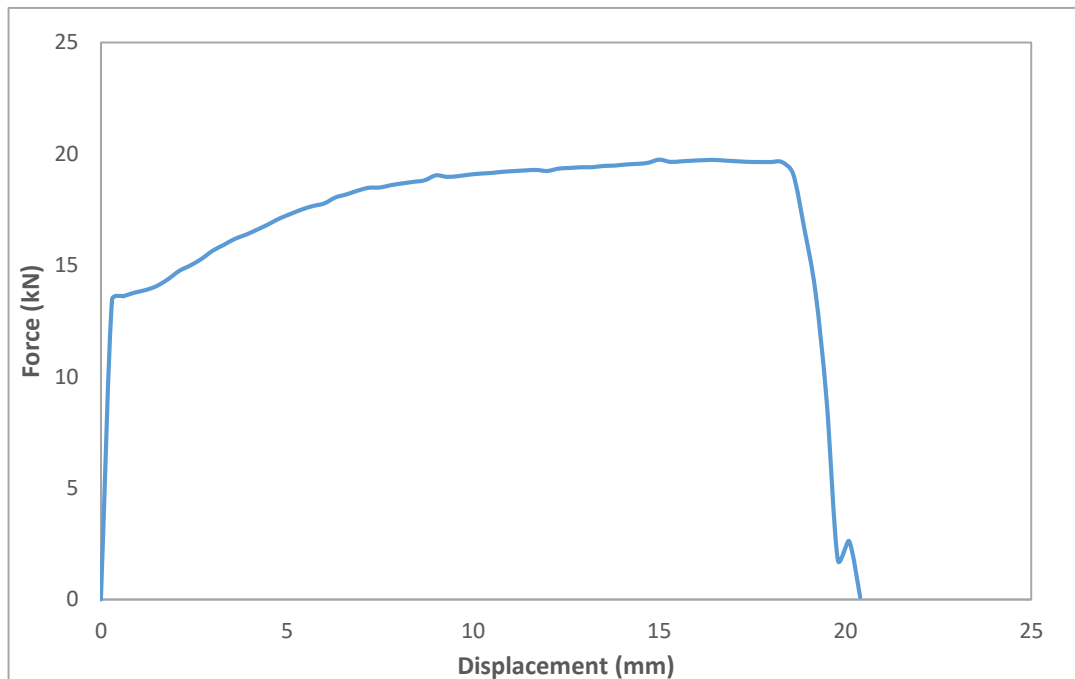


**Figure 3.11.** Force-displacement history of the specimen.

Figure 3.12, given below, shows the strain vs. damage history of an element from the specimen. It is apparent that once the strain value crosses this fracture strain (which in this model has been set to 0.34), the material starts to degrade and lose its capacity. The material continues to lose its capacity in a linear fashion due to the presence of progressive ductile damage until the stiffness of an element gets completely degraded.

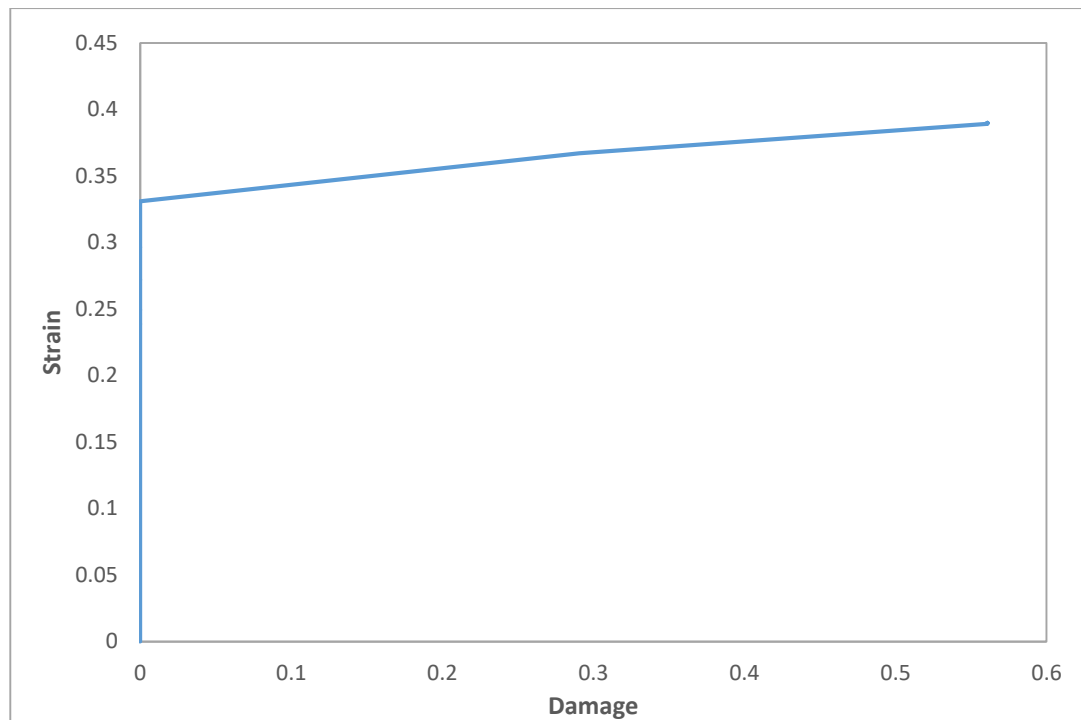


**Figure 3.12.** Strain vs. damage history of an element in the specimen.

Finally, as shown in Figure 3.13 a comparison was made based on stress-strain history between the experimental results and the results obtained from Abaqus. It can be noticed that the curve obtained from Abaqus is very much identical to the curve obtained from the experiment, thus proving the validity of this material model.

Therefore, the experimental results and Abaqus results are in good agreement with each other and the damage initiation criterion, which is necessary for observing the fracture in the elements, is working effectively without any problems. Therefore, it can be said that the material model used in this thesis is safe to use for further simulations.

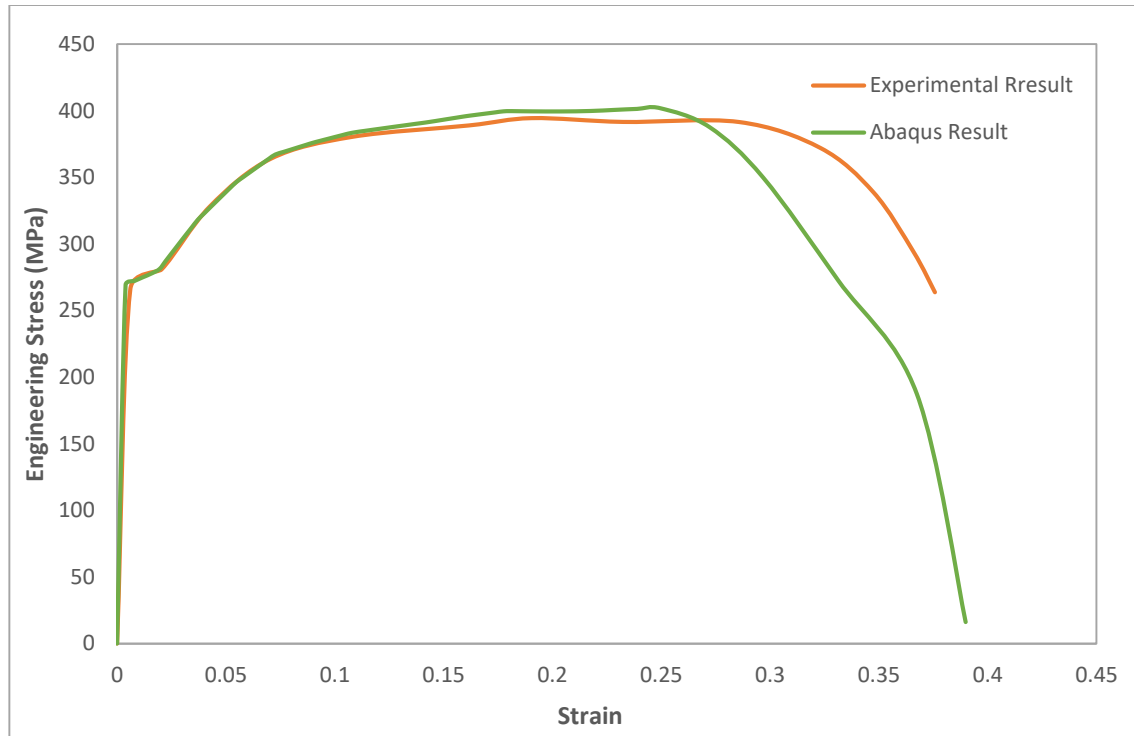


**Figure 3.13.** Stress-strain comparison between experimental results and Abaqus results.

### 3.2.2.2 Transmission Tower Sections

Abaqus has a section module where information about the properties of parts is assigned. Various sections can be assigned to different parts of a model, depending on the type of region. In this work, beam sections are assigned to the whole transmission tower because it is suitable for structures with cross-section smaller as compared to the length. So for the whole tower model, four beam sections have been defined having four different L profiles and then assigned with the material property as mentioned in the previous topic. After defining sections, they are allocated to the transmission tower at different locations, such as in the main leg member, horizontal members, diagonal bracings, and cross arms. The convenient way of doing this is by creating the sets for the members with the same cross-section and then assigning the section properties. By doing this, it is possible to make changes in the set of selected members with just a click instead of wasting time by selecting all members one by one.

**Table 3.3** Transmission tower section profiles

<b>Profiles</b>	<b>Assigned Region</b>
L150*12	Bottom legs
L110*8	Middle legs
L90*6	Arms, Bottom bracing
L50*4	Top legs, Top bracing, Middle bracing

### **3.2.3 Step Module**

In this thesis dynamic explicit procedure has been used for carrying out the investigation of collapse mechanism of transmission tower. Dynamic explicit is a special type of solution procedure that is used for solving highly non-linear problems and can also show the precise representation of collapse process of any structure. Explicit procedure works with central difference method (CDM) for integrating the equation of motion explicitly throughout the time. With the passage of each increment, CDM uses initial kinematic conditions for computing the kinematic conditions for the following increment and can also execute a large number of small-time increments in an efficient manner. Few advantages of using this type of analysis solver are:

1. This solver is computationally efficient for carrying out analysis of big complicated models with short dynamic response time or for the analysis of highly discontinuous circumstances.
2. Dynamic explicit solver uses large deformation theory under which it is possible to catch large deformations and large rotations experienced by the structural model.
3. Dynamic explicit analysis can be used for all element types available in Abaqus.
4. The explicit solver allows users to choose between automatic and fixed time incrementation. Abaqus chooses automatic time incrementation on default settings.

Since the progressive collapse analysis of transmission tower will be carried out in this work, which is a very complex and large structure, therefore, it is reasonable to choose explicit dynamic procedure because of having low CPU cost.



### 3.2.3.1 Step

Splitting the problem history into steps is one of the fundamental concepts in Abaqus. A step is any appropriate phase of history, which in its most basic form can be static analysis. A step is defined in Abaqus for conducting the following tasks:

1. **Creating Analysis Step:** Inside the Abaqus step menu, the assignment of one or more analysis steps is done to record the changes in loads, changes in interactions of different members with each other, changes in boundary condition and any other changes that might take place in the structural modal while analysis is running. In addition, specifying the type of analysis procedure (static general, dynamic implicit, dynamic explicit, heat transfer), defining the increment size (each step is divided into many increments) and indicate if geometric nonlinearity \*NLGEOM is to be taken in consideration or not is done in this module.
2. **Defining Output Requests:** The purpose of defining output request is to obtain the required variables such as displacements, stresses, strains, and forces of a model and to define the rate at which these variables will output from the analysis. The values of these variables are computed after each step increment.

In this study, an earthquake step was created in the step module using Dynamic, Explicit procedure for solving all calculations in the analysis under the influence of seismic loads. The reason for choosing explicit procedure is that this procedure is better for solving highly non-linear problems, and it can also include the failure of a member due to material degradation such as ductile failure, which is used in this model. Since the loads on the transmission tower will create large displacement effects, therefore geometric nonlinearity was included in the calculations by turning on Nlgeom. The total duration of this step was set to 20 seconds because the transmission tower was also simulated under earthquake loads for 20 seconds. Incrementation type for this step was selected as Automatic, Abaqus then chooses appropriate increment size itself as analysis continues.

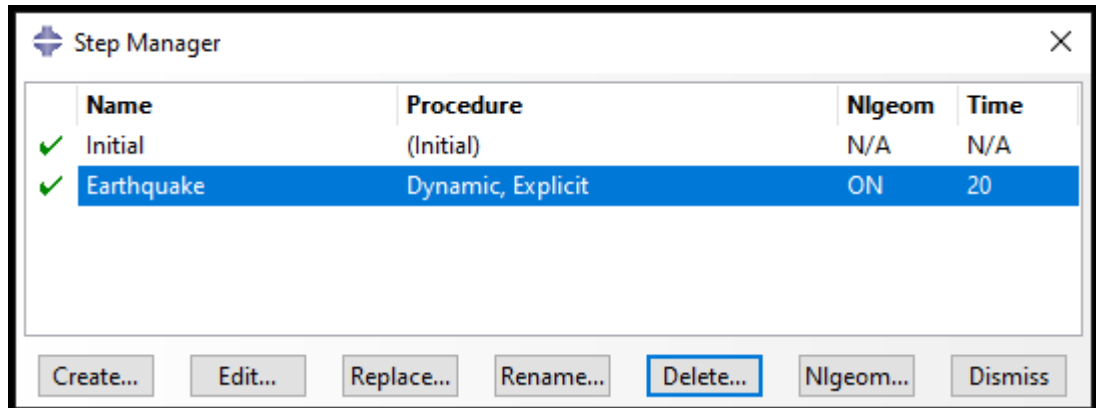


**Figure 3.14.** Picture representing the steps considered in seismic analysis.

In addition to the default output variables that are selected automatically in Field Output request manager, some extra output requests were made for the earthquake step which are given below:

DMICRT: Damage initiation criterion, for indicating the initiation of damage in material.

SDEG: Scalar stiffness degradation, for indicating if the material is completely degraded or not by showing '1' for completely degraded and '0' for undegraded.

The frequency at which the explicit solver will create the output was assigned with 'Every x unit of time' option, where the value of x was set to = 0.02. It means that after every 0.02 second time increment, Abaqus will create the output of all defined variables.

### 3.2.4 Load Module

#### 3.2.4.1 Loads

The load computation on a structural model in Abaqus is done by entering the acceleration magnitude present inside the gravity load definition module and by entering density that is present inside material module.

Therefore, for the non-linear dynamic analysis of transmission tower, gravity load has been assigned for the whole transmission tower inside the load module under the Dynamic, Explicit step. To define the constant acceleration due to gravity in vertical direction, Component 3 was specified with the value of  $-9.81\text{m/s}^2$ .

### 3.2.4.2 Calculation of Wind Load

Wind load is calculated as per Indian standard code of practice for buildings and structures IS 875 part 3 and assigned as lateral force acting on every panel of the transmission tower. Wind load calculation on transmission tower has proceeded in the following manner:

$$\text{Basic wind speed } (V_b) = 44 \text{ m/s}^2$$

$$\text{Wind Zone} = 3$$

$$\text{Terrain Category} = 2$$

$$\text{Conversion factor } (K_0) = 1.375$$

$$\text{Risk Coefficient } (K_1) = 1.11$$

$$\text{Terrain Roughness Coefficient } (K_2) = 1$$

$$\text{Reference wind speed } (V_R) = \frac{V_b}{K_0} = \frac{44}{1.375} = 32$$

$$V_R = 32 \text{ m/s}$$

$$\text{Design wind speed } (V_d) = V_R * K_1 * K_2 = 32 * 1.11 * 1 = 35.52$$

$$V_d = 35.52 \text{ m/s}$$

$$\text{Design wind pressure } (P_d) = 0.6 * V_d^2 = 0.6 * (35.52)^2 = 757$$

$$P_d = 757 \text{ N/m}^2$$

$$\text{Wind load acting on each tower panel } F_w = P_d * C_{dt} * A_e * G_t \quad (3.1)$$

Here,

$A_e$  = Effective area of the panel.

$G_t$  = Gust response factor for the tower, depends on height above ground.

$C_{dt}$  = Drag coefficient pertaining to wind blowing against the face of tower. The value of  $C_{dt}$  depends on the solidity ratio.

Starting from the bottom of transmission tower, the lowest panel close to the ground has been named A, and following panels in upward direction have been named in

alphabetically ascending order. Solidity ratio is calculated for every individual panel of transmission tower with Equation 3.2 given below, and then the drag coefficient is found as per IS 875 part 3.

$$\text{Solidity Ratio } (\phi) = \frac{\text{Projected area of all individual elements}}{\text{Area enclosed by the boundary of frame normal to the wind direction}} \quad (3.2)$$

**Table 3.4.** Solidity ratio and drag coefficient for various panels of transmission tower.

<b>Panel Number</b>	<b>Solidity Ratio (<math>\phi</math>)</b>	<b>Drag Coefficient (<math>C_{dt}</math>)</b>
A	0.065	3.4
B	0.071	3.4
C	0.080	3.4
D	0.089	3.4
E	0.122	2.9
F	0.108	2.9
G	0.107	2.9
H	0.124	2.9
I	0.133	2.9
J	0.147	2.9
K	0.17	2.9
L	0.143	2.9
M	0.116	2.9
N	0.143	2.9
O	0.143	2.9
P	0.116	2.9
Q	0.143	2.9
R	0.143	2.9
S	0.143	2.9

The wind load was calculated for each tower panel after obtaining all the parameters required as per Equation 3.1. The wind load on each panel is given in the table below:

**Table 3.5.** Wind load acting on various panels of transmission tower.

<b>Panel Number</b>	<b>Wind Load (<math>F_w</math>)</b>
A	33652 N
B	20384 N
C	20158 N
D	20127 N
E	11613 N
F	4583 N
G	4741 N
H	4109 N
I	3898 N
J	3688 N
K	3213 N
L	3103 N
M	2504 N
N	3103 N
O	3103 N
P	2504 N
Q	3103 N
R	3190 N
S	3190 N

The wind loads calculated in this section were assigned to all the panels of tower as shown in Figure 3.15. Transmission tower was simulated with dynamic explicit analysis for 10 seconds by keeping all translational and rotational movements of the base nodes fixed.

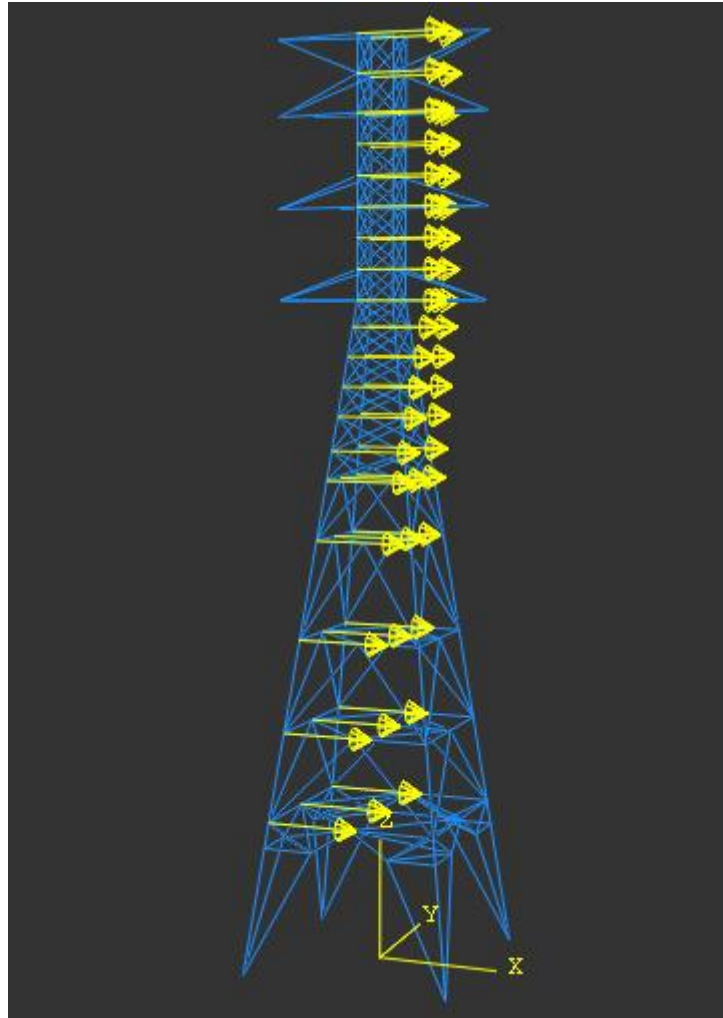


**Figure 3.15.** Wind load acting on various panels of transmission tower.

### **3.2.4.3 Amplitude for Seismic Load**

The purpose of creating the amplitude in Abaqus is to define time variation of load, acceleration, displacement, or any other variable to be assigned during a step or for the complete duration of analysis. There are different ways to create amplitude, such as by defining digitized acceleration-time history record of an earthquake or by inputting mathematical equations like sinusoidal variation.

An amplitude curve of El Centro earthquake record as explained in next unit (3.2.4.4), was used to define the variation of acceleration with time in the tabular form in ABAQUS. The time difference between every increment was set as 0.02 sec.

### 3.2.4.4 Seismic Loads Acting on Lattice Tower

In this work, El Centro north-south time history accelerograms has been used for simulating the transmission tower under seismic loads. El Centro is a town in California, USA, which experienced a massive earthquake in 1940, resulting in the deaths of many people and damaging almost 80% of the buildings in that area. This seismogram is regularly used in the design of earthquake resisting structures these days, and especially used for time history analysis method.

The peak ground acceleration of El Centro earthquake lies in 2.02 seconds therefore, to reduce the overall time of analysis, it was more logical to take only first 20 seconds of El Centro N-S accelerogram in the simulation. The accelerogram of this earthquake is shown in Figure 3.16.

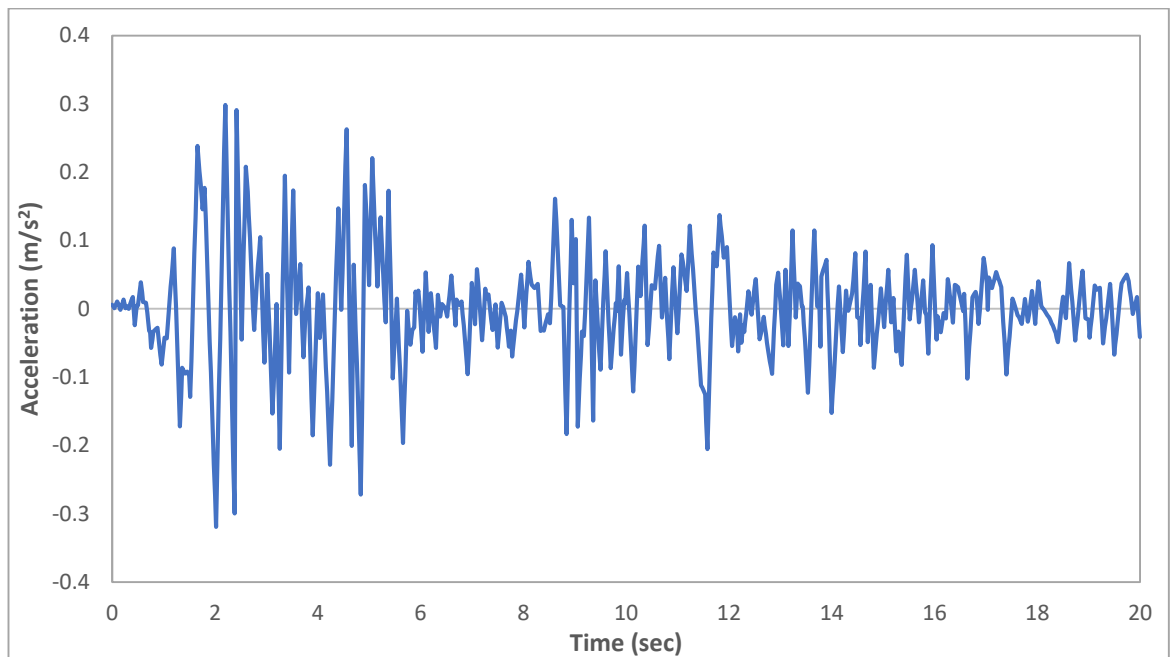


**Figure 3.16.** El Centro N-S accelerogram.

### 3.2.5 Boundary Conditions

Abaqus allows its user to generate the different boundary conditions for a model and gives authority to control them under various steps by applying different loads. Boundary

conditions of a model can be defined in various forms, such as by specifying the degree of freedoms, displacements, accelerations, and velocities at nodes or parts. It is necessary to specify the step in which the boundary condition needs to be activated (Abaqus 2014). In this study, two types of boundary conditions were assigned to the base nodes of transmission tower, which are explained below:

1. Fixed Boundary Condition: In this case, displacements and rotations at the base nodes of transmission tower were restrained in all directions (x,y,z), which means all degrees of freedom were kept zero. This restriction was done by selecting ENCASTRE  $U1=U2=U3=UR1=UR2=UR3=0$  boundary condition in the Initial step.
2. Acceleration boundary condition: An acceleration boundary condition has been defined by assigning the El Centro N-S amplitude data to the base nodes of transmission tower. This amplitude was applied in the transverse direction of the tower under earthquake step and then by selecting 'Acceleration/Angular acceleration' type boundary condition.

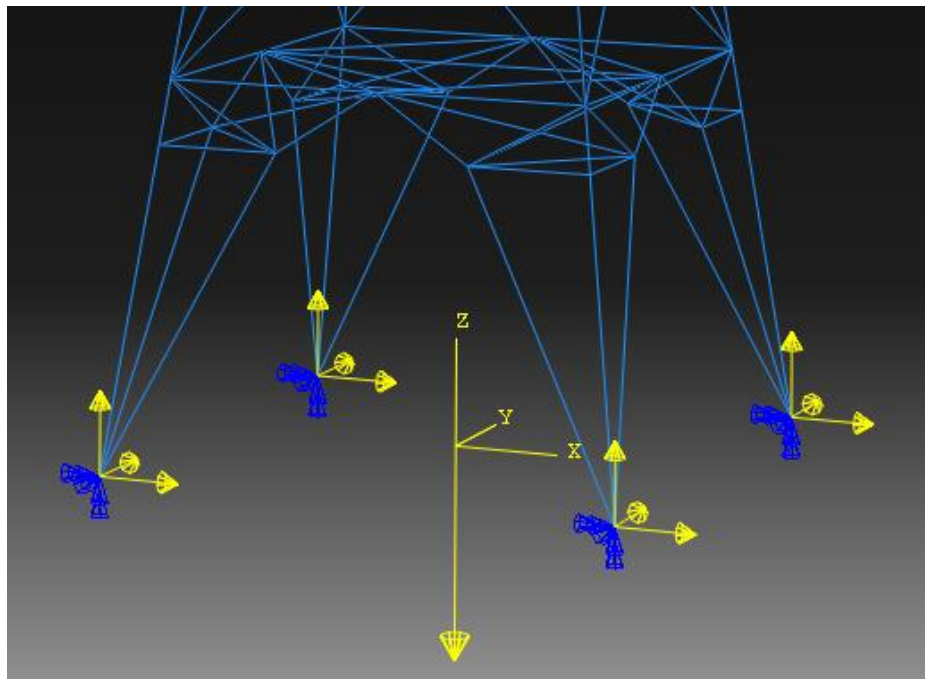


**Figure 3.17.** Acceleration boundary condition of transmission tower.



### 3.2.6 Interaction Module

Connections in Transmission Tower:

For choosing the suitable type of connections in transmission tower, literature review was done on previous researches, and the most relevant connection was chosen.

1. Rao et al. (2001) stated that the traditional way of representing the connection between different members in the steel lattice tower is with a hinge joint. However, it is not the actual representation of real joint behavior. An assumption is made while assigning hinged joints on steel lattice tower that all the members are connected with each other concentrically such that only and only axial forces are carried in the angle sectional members while analyzing the tower. But in reality, this assumption does not hold true as leg members and bracing members are not loaded axially because of various reasons such as:

- The joints present in the main leg members are continuous most of the time.
- In most of the connections, the joint is made of more than one bolt therefore, the joints are semi-rigid.
- The force transfer in lattice tower appears to be eccentric in nature because bolt connection is made only through one leg of angle member.

All the facts provided above proved both axial forces and bending moments take place in the angle members of lattice tower.

2. Tian et al. (2015) used a rigid connection between the transmission tower members for observing non-linear seismic behavior under earthquake loading.
3. Hamada et al. (2010) assigned the rigid connections between the members of transmission tower. They did this by assuming multi-bolted connections that are able to transfer moments under wind loadings.
4. A numerical failure analysis was conducted by Tian et al. (2019), where they suggested using rigid joints in the lattice steel transmission tower.
5. Full scale tests were conducted on steel transmission tower by Jian et al. (2011) to study the effect of connections. They came to the conclusion that it was more precise to predict the behavior of tower with a fixed connection than with pinned connection.

After all the literature review and arguments, it was decided that the connections between various members of transmission tower studied in work to be assumed as multiple-bolted and welded. These connections are considered as rigid because of the fact that the rotational restraint provided by them are very large in magnitude.

### **3.2.7 Mesh Module**

Meshing is a technique that gives users the freedom to generate meshes on parts or assemblies of a model made in Abaqus. The type of mesh attributes needed for the analysis can be controlled by the users with different options available in the program (Abaqus 2014).

The whole transmission tower used in this thesis has been assigned with Local Seeds by number, and every member of the tower was selected as one mesh element. After meshing the part instance, the model needs to be assigned with proper element type. There are various types of elements available in the Abaqus library, but the most appropriate element type for the transmission tower members is B31 first order three-dimensional beam element.

### **3.2.8 Job Module/ Solution**

All the steps taken in Abaqus program where the model of the physical problem has been defined is called preprocessing. Once the preprocessing of finite element model (for example defining the geometry, material properties, loads, boundary conditions and mesh) is completed, the model is written in finite element code and then transferred to the solver (ABAQUS/Explicit) present in the job module to analyze the model. Abaqus creates an input file of the model after job is submitted for analysis and after that solver carry out the analysis by utilizing the contents of input file. The simulation generally operates as a background activity where the solution process of the numerical problem specified in the model is done.

Once the job has been submitted for analysis, “Monitor” option available in the job manager allows users to monitor the progress of analysis by providing continuously updated information regarding log, errors, warnings, and output.

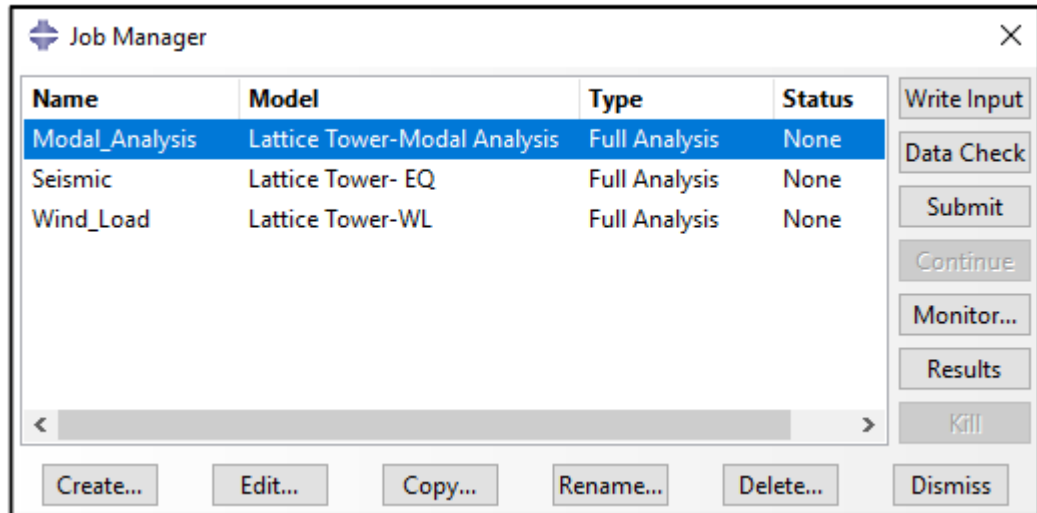


**Figure 3.18.** Various jobs in Abaqus ready for simulations.

### 3.2.9 Visualization Module/ Postprocessing

Once the simulation is completed, the output database (such as displacements, stresses and other variables) that was requested from output request in Step module can be evaluated. This evaluation process popularly known as postprocessing is done in visualization module.

Visualization module in Abaqus provides a platform to display the graphical result of analysis results as well as helps in reading the output database that was created throughout the course of analysis. There are various ways by which the finite element model and its results can be generated, such as Undeformed shape, Deformed shape, Contours, Time history animation and X–Y data.

The simulation results in form of shape of a model, graphics, and output database is given in Chapter 4 (Result and Discussion) of this thesis.

## 4. RESULTS AND DISCUSSION

In this chapter, the results of the analyzes made using the materials and methods explained in the previous section are mentioned. All the graphs obtained during the investigation of damages caused due to wind load and seismic loads on the transmission tower is given in this chapter.

### 4.1 Free Vibration Analysis and Damping

It is very important to take damping of a lattice tower into consideration while conducting explicit analysis to attain maximum dynamic forces. The most common method to do that is by using Rayleigh damping in dynamic analysis. Prior to Rayleigh damping, natural frequencies of transmission tower are found by performing modal analysis. The subsections given below presents the free vibration analysis of the tower followed by damping.

#### 4.1.1 Free Vibration Analysis of Transmission Tower

Natural frequencies of transmission tower were determined by running free vibration analysis in Abaqus program. Figure 4.1, figure 4.2, and figure 4.3 belonging to the transmission tower model illustrates the bending and twisting mode shapes for first three notable frequencies. It is required to conduct free vibration analysis of a modal because the tower would collapse if the frequency of tower under excitation loadings will match(reach) the natural frequency of tower.

**Table 4.1.** Natural frequencies belonging to notable bending and twisting modes of the transmission tower.

Frequency Mode	Type of Mode	Frequency (rad/s)
1	Bending	2.09996
2	Bending	2.1992
3	Twisting	4.0674

4	Bending	5.4406
5	Bending	5.9837

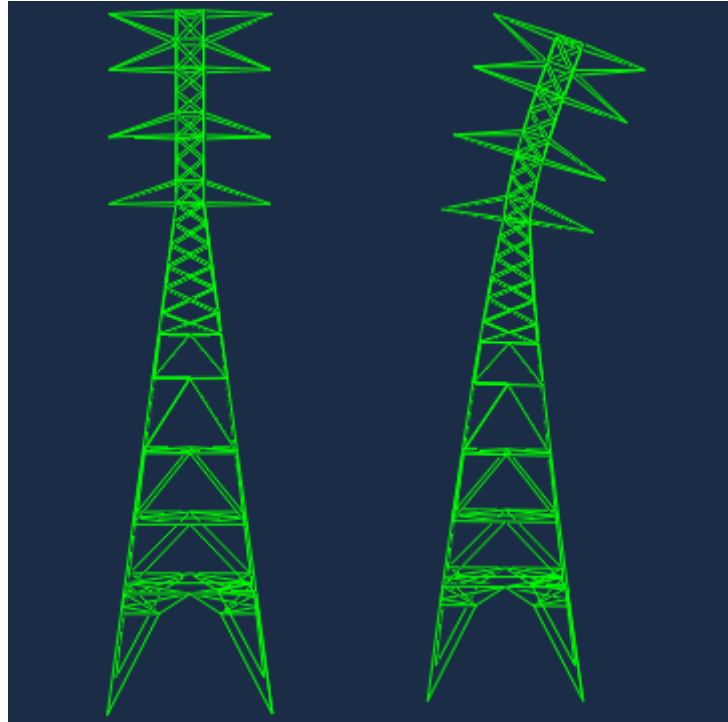


**Figure 4.1.** Mode 1 of transmission tower.

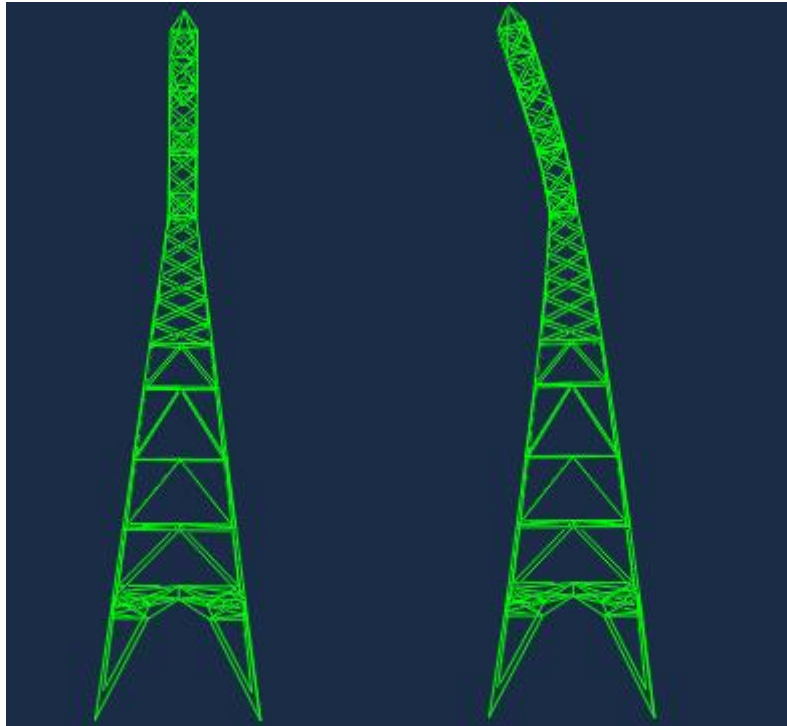


**Figure 4.2.** Mode 2 of transmission tower

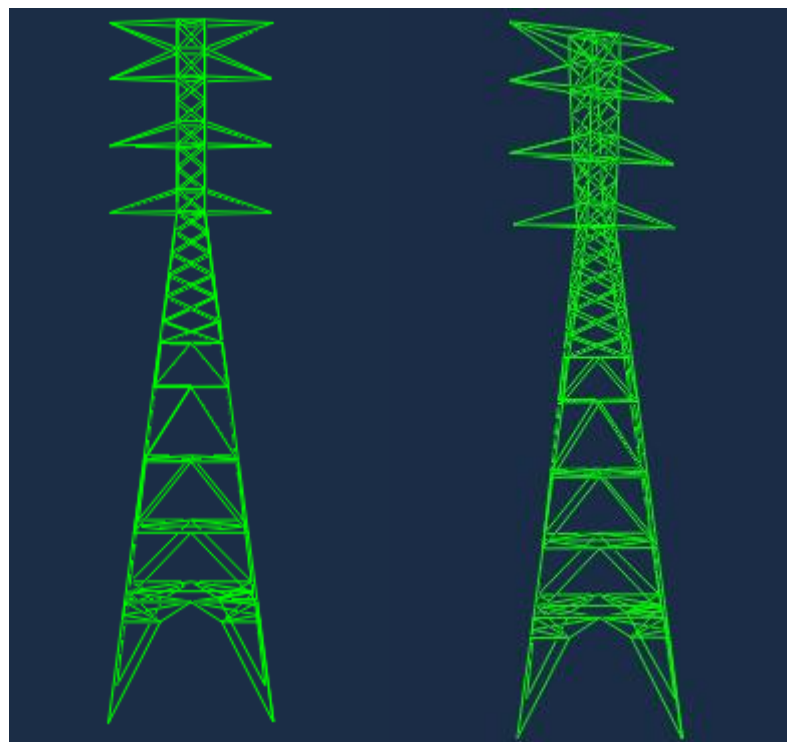


**Figure 4.3.** Mode 3 of transmission tower

### 4.1.2 Verification of Finite Element Model

The modal analysis result obtained from Abaqus program pertaining to the transmission tower was verified by running the modal analysis of same structure in SAP2000 program. It was found that the natural frequencies of tower obtained from SAP2000 modal analysis were very much close to the natural frequencies obtained from Abaqus. The comparison of first three natural frequencies of tower obtained from Abaqus and SAP2000 are given in the table below.

**Table 4.2.** Comparison of frequencies between two programs.

Mode	Abaqus	SAP2000	% difference
1	2.09996	2.11789	0.85%
2	2.1992	2.2173	0.81%
3	4.0674	4.10843	1%

It can be clearly seen from the table above that the difference between the results of natural vibration frequencies is within an acceptable range, which is less than 1%. Even the mode shapes obtained from two programs are exactly the same, which proves the accuracy of the model.

### 4.1.3 Damping

In the non-linear analysis of structures especially in dynamic analysis, damping plays a major role. One of the most efficient ways to treat the damping in a structure is with the help of Rayleigh damping equation in the form of

$$[C] = \alpha[M] + \beta[K] \quad (4.1)$$

Here,

[C] = Damping matrix of a physical system

[M] = Mass matrix of a physical system

[K] = Stiffness matrix of a physical system

$\alpha$  = Mass proportional Rayleigh damping, damps lower frequencies

$\beta$  = Stiffness proportional Rayleigh damping, damps higher frequencies

The relationship between damping coefficients  $\alpha$  and  $\beta$ , and fraction of critical damping  $\xi$  for a given mode  $i$  can be expressed as:

$$\xi_i = \frac{\alpha}{2\omega_i} + \frac{\omega_i\beta}{2} \quad (4.2)$$

Where,  $\omega_i$  is the natural frequency of the system, for the  $i^{\text{th}}$  mode of vibration.

The value of mass proportional Rayleigh damping coefficient can be calculated from the following equation:

$$\alpha = \frac{2\omega_1\omega_2}{\omega_2^2 - \omega_1^2} (\xi_1\omega_2 - \xi_2\omega_1) \quad (4.3)$$

And the value of stiffness proportional Rayleigh damping coefficient can be calculated from:

$$\beta = \frac{2(\omega_2\xi_2 - \omega_1\xi_1)}{\omega_2^2 - \omega_1^2} \quad (4.4)$$

### **Computation of damping constants ( $\alpha$ and $\beta$ ) of transmission tower.**

In this thesis, the critical damping ratio for transmission tower was taken as 2%. Stiffness proportional damping was ignored because Abaqus/Explicit decreases stable time increment sharply if stiffness proportional damping is taken into consideration, which can lead to longer analysis time. Therefore, only mass proportional damping has been used in this thesis. Modal analysis was done in Abaqus to extract the first two values of natural frequency. Since transmission tower has large degrees of freedom so only first few modes



contribute to the dynamic behavior. Therefore, the first two natural frequencies of transmission tower obtained from modal analysis are given below in Table 4.3.

**Table 4.3.** First two natural frequencies of transmission tower.

$\omega_1$	$\omega_2$
2.0996	2.1992

The mass proportional damping coefficient was calculated as given in the equation 4.3 above with the help of already determined natural frequencies of system ( $\omega_1$  and  $\omega_2$ ) along with the critical damping ratio ( $\xi$ ) of 2%.

The calculated mass proportional damping was found to be equal to  $\alpha = 0.269$ . This damping value is applied to all the elements in model having mass. The calculated mass proportional damping was assigned to the tower in the material property option as Alpha damping.

## 4.2 Wind Load on Transmission Tower

This part is focused on investigating the damages in transmission tower when subjected to wind loads. As discussed previously in section 3.3.1, the wind loads acting on the different panels of transmission tower were calculated and then assigned accordingly. After that, the tower modal was analyzed for the duration of 5 seconds while keeping material and geometric nonlinearity active.

The nonlinear wind response analysis was completed without the collapse of the structure. However, during analysis, small plastic strains were observed in a few members of the transmission tower. Figure 4.4 below illustrates the time-history curve of top horizontal displacement of a transmission tower in X direction. The maximum displacement recorded at the top of the tower was 0.66m.

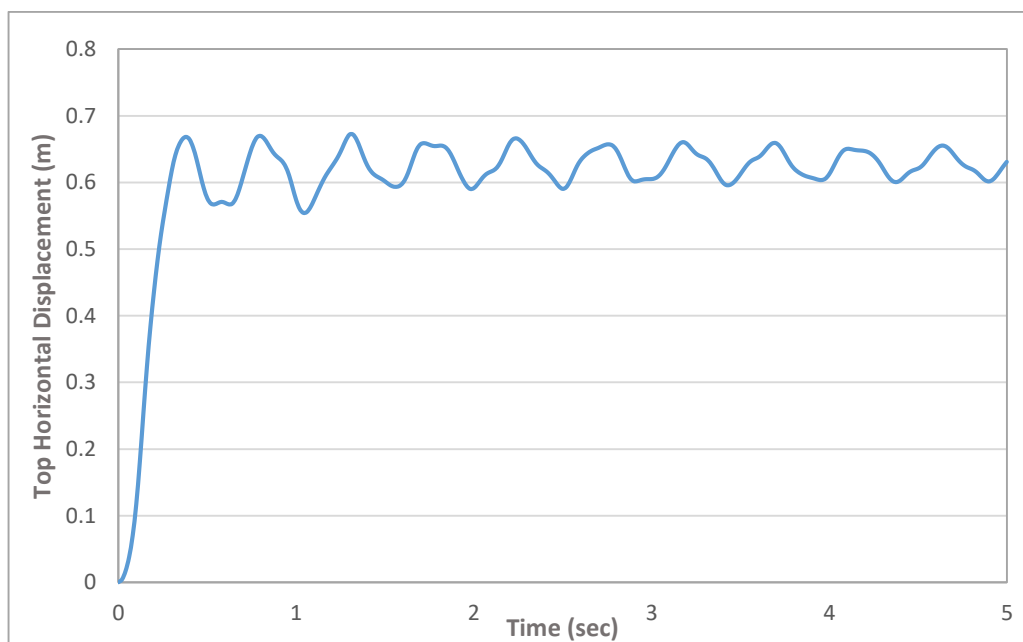


**Figure 4.4.** Displacement time history of the tower top.

As stated in Code for Design of High-Rising Structures (2006), horizontal displacement at the top of the tower should be limited to 1/50 of its elevation in nonlinear analysis. The

total height of transmission tower model in this work is 54.8m. Therefore, the maximum displacement recorded at tower top (0.66m) is within the range of displacement limits. The maximum equivalent plastic strain (PEEQ) recorded at the end of analysis was found in element 119 of tower leg member in panel M. This plastic strain value was almost 0.0134, which is a very small number to initiate the damage in an element.

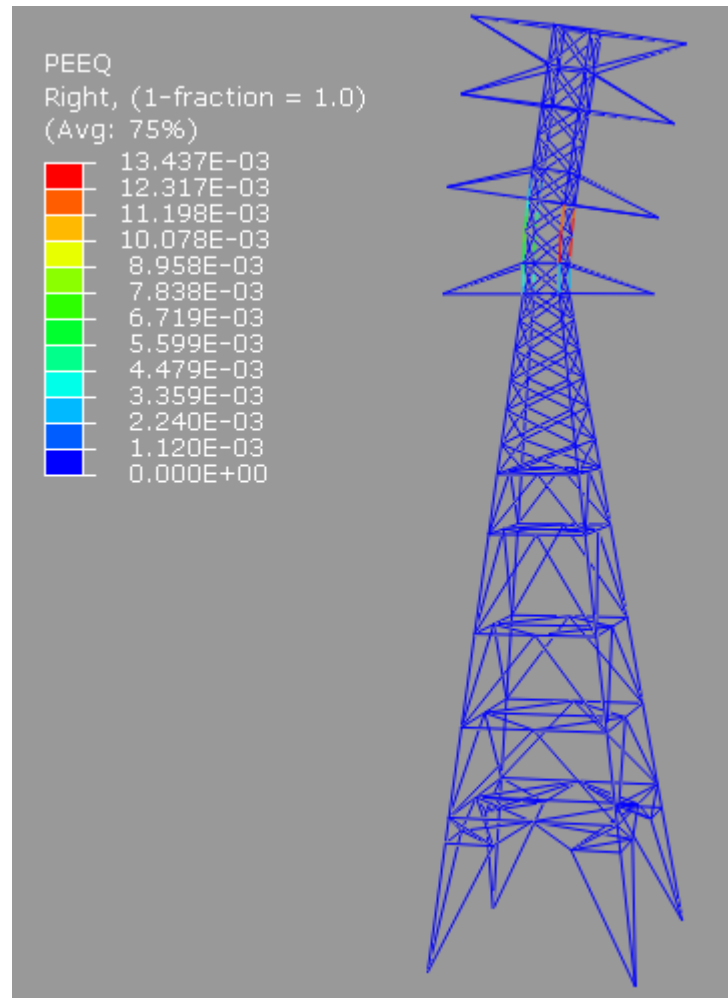


**Figure 4.5.** Members with plastic strain in transmission tower.

The development of plastic strain in element 119 over the period of time is shown in Figure 4.6. Plastic strain in element 119 started after 0.16 seconds as soon as the stress component (S11) reached the yield stress value of 264 MPa. Shortly after crossing the yield stress, the plastic strain in the element kept on increasing sharply until 1.32 sec, after which it became stable with no increase.

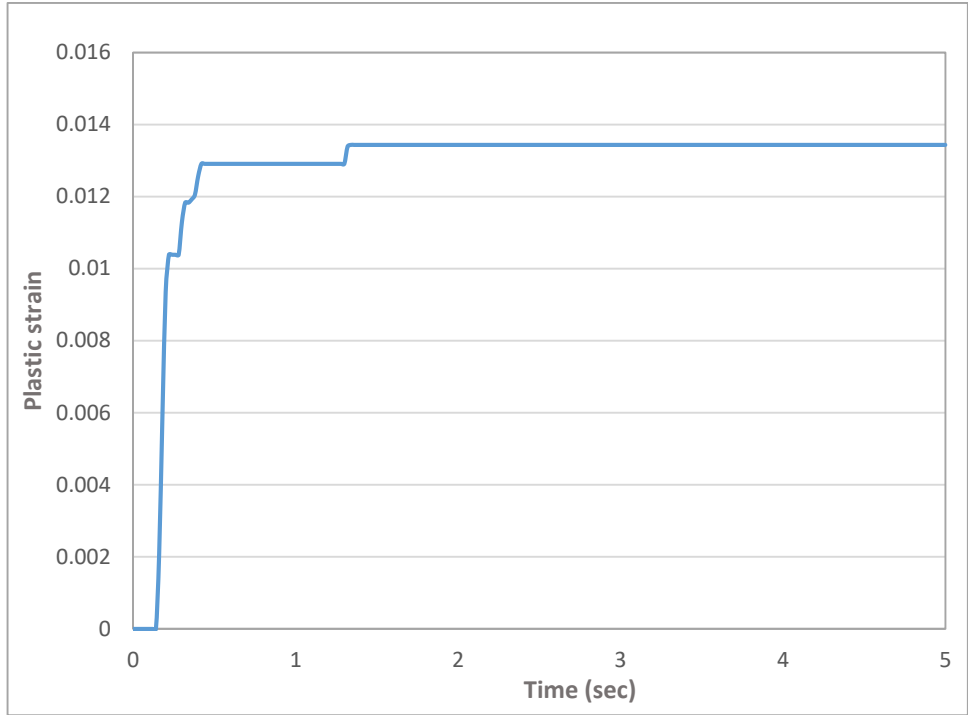


**Figure 4.6.** Plastic strain time-history curve of element 119.

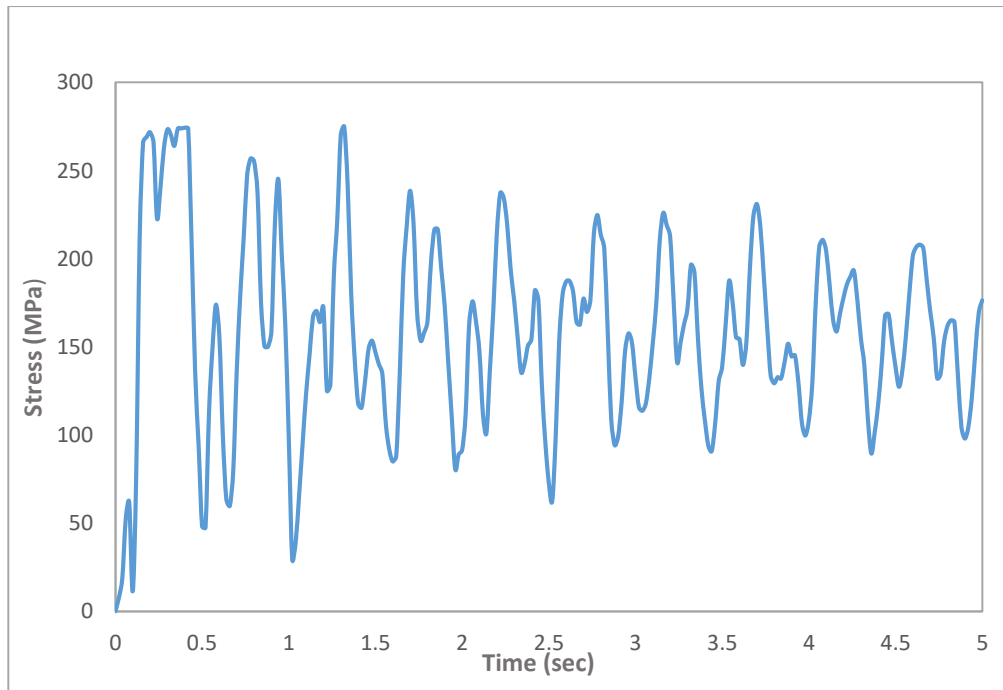


**Figure 4.7.** Stress time history of element 119.

The value of ductile damage initiation criterion (DUCTCRT) for element 119 at the end of analysis was found as 0.141. This value can be verified by hand calculations using Equation 3.5 as explained in chapter 3,

$$\Delta\omega_D = \frac{\Delta\bar{\varepsilon}^{pl}}{\bar{\varepsilon}_D^{pl}(\eta, \bar{\varepsilon}^{pl})}$$

$$\Delta\omega_D = \frac{0.0134}{0.0948} = 0.141$$

The stiffness degradation of material would have only started if the damage index ( $\Delta\omega$ ) reached the value 1, but it didn't reach. Therefore, this indicates the presence of very slight damage in the element, which is not a major risk of concern. Hence no element lost its load-bearing capacity in this wind load analysis.

The result of this analysis concludes that panel M is the critical region of transmission tower under wind loads, and in case of such wind loads the damage position of structure is most likely to appear in this panel. It is also concluded that the maximum top displacement of tower is within the range of displacement limits, and no element lost its bearing capacity, which didn't cause internal force redistribution within the structure; thus, the whole structure remained stable.

#### **4.3 Effect of increasing the wind speed on the tower**

As seen from the result of previous wind load analysis, it was clear that the tower withstood the wind loads with negligible damage. Therefore, in this analysis, the transmission tower was subjected to the highest wind loads permitted by the codes with the aim of capturing the damages and study the response of tower.

The new wind loads were calculated by increasing the basic wind speed to 55m/s. The new wind speed (55m/s) is 25% more than the previous wind speed (44m/s). Each panel of transmission tower was assigned with the new calculated wind loads in the same way

as done in the previous wind load analysis which had a basic wind speed of 44m/s. New wind loads on different panels of a transmission tower are given in table 4.4.

**Table 4.4.** New calculated wind loads after increasing the wind speed.

<b>Panel Number</b>	<b>Wind Load (<math>F_w</math>)</b>
A	55569.6 N
B	33660 N
C	33286 N
D	33235 N
E	19176.2 N
F	7569 N
G	7830 N
H	6786 N
I	6438 N
J	6090 N
K	5307 N
L	5124 N
M	4135 N
N	5124 N
O	5124 N
P	4135.4 N
Q	5124.3 N
R	5268.9 N
S	5268.9 N

The non-linear wind load analysis was completed after 5 seconds. The final shape of tower after the completion of analysis is given in Figure 4.8. It can clearly be seen that the majority of plastic strain is accumulated in the vertical members of panel M in the top section of transmission tower. It is to be noted that in the previous analysis having low

wind loads, the plastic strain also took place in the same area of tower as in this new wind load analysis.

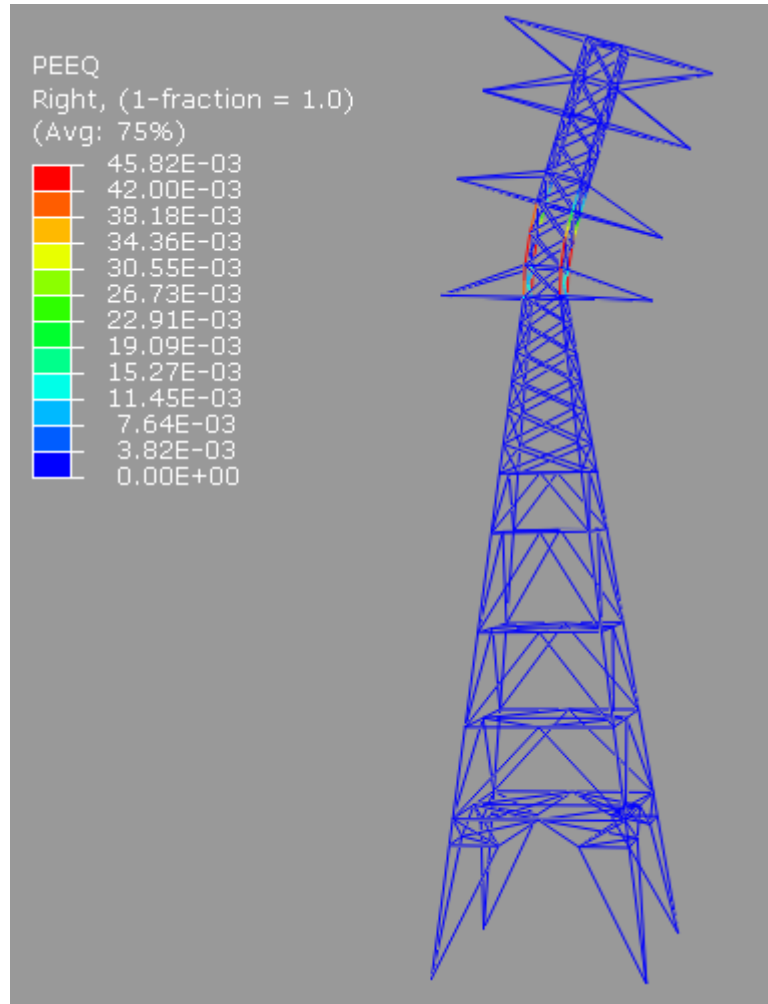


**Figure 4.8.** Plastic strain on the various members of the transmission tower.

The result from this analysis shows that the plastic strain (PEEQ) values have increased subsequently with the increase in wind loads on the tower. The maximum PEEQ value recorded in this analysis is 0.0458, whereas the max. PEEQ value in the previous analysis was 0.0134. On comparing the plastic strain developed in tower members from two different analyses, it was noticed that there has been 71% increase in plastic strain (PEEQ). The graphical visualization of the comparison of strain values for element 119 is given in Figure 4.9.

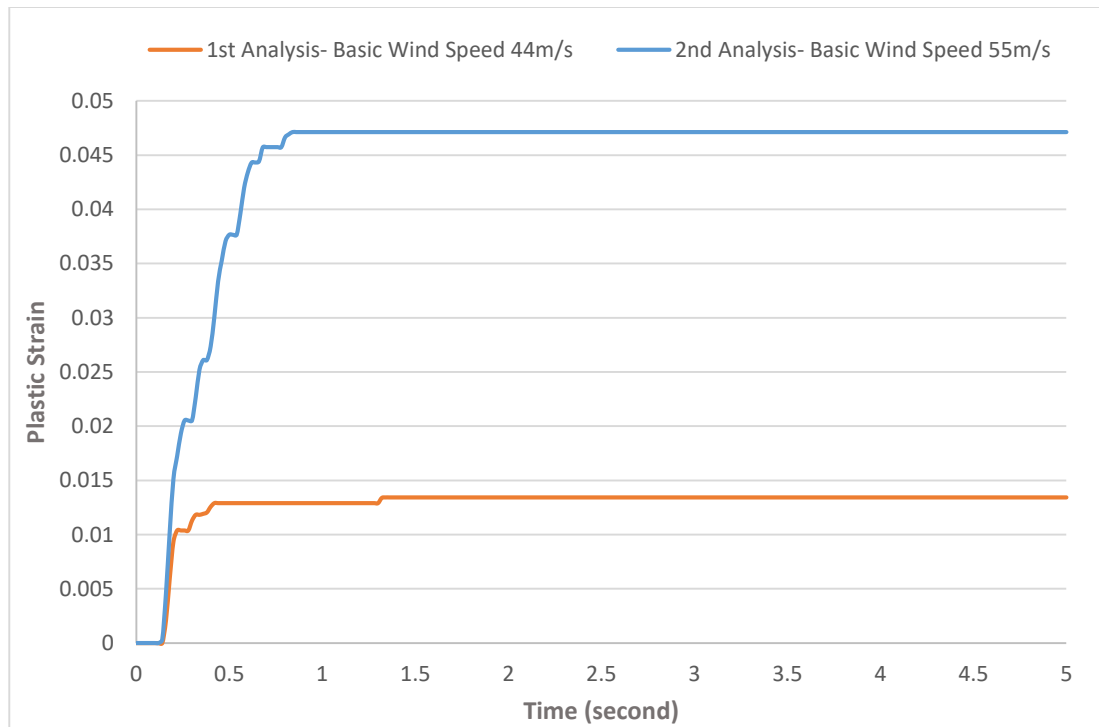


**Figure 4.9.** Comparison of plastic strain values obtained from two wind load analysis.

From Figure 4.9, it is visible that there is a surge in plastic strain between 0.14 and 0.86 seconds in the second analysis. The reason for this surge in the plastic strain value is high-intensity forces acting on the members of tower, which in turn results in high stresses. Plasticity started soon after the stress value crossed the yield stress of 264 MPa. The stress in the member kept on increasing after it crossed the yield stress mark, subsequently increasing the plastic strain values until 0.86 seconds. After 0.86 seconds the stress value started to decline below the yield stress, thus keeping the plastic strains constant until the end of analysis. The graphical representation for comparing the stresses in the element 119 during two analyses are given in Figure 4.10.



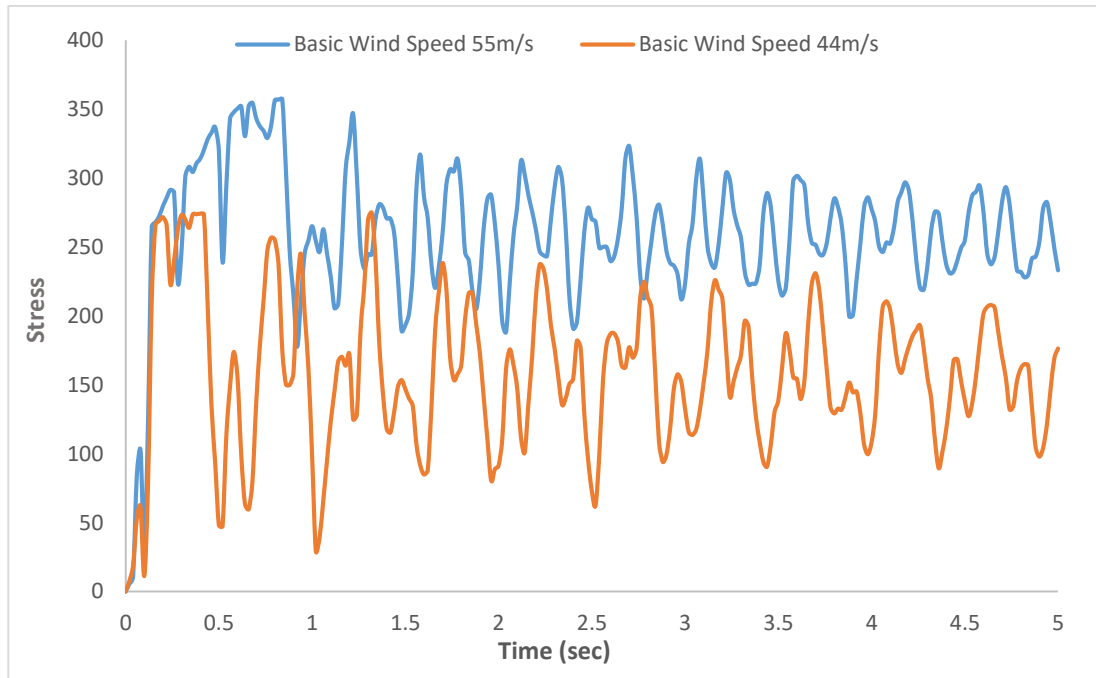


**Figure 4.10.** Stress time history of the element under wind loads.

From the stress comparison given in Figure 4.10. it can be seen that the maximum stress developed on element 119 in the first analysis was 274.2 MPa, and in the second analysis it jumped to 357.2 MPa. The obvious reason for this significant difference in maximum stresses in two analyses is the increase in the wind loads. The percentage increase of the maximum stresses in the two analyses is 30.2%.

A better graphical representation of the history of stress vs. plastic strain on the element 119 is given in Figure 4.11. It can be evaluated from the graph that once the stress value crosses the yield stress mark, the plastic strain starts and then keeps on increasing or remains constant depending on the stress values. If the stress value is more than the yield stress, the plastic strain will increase; otherwise, it will remain constant. It can also be noticed from the graph that the value of plastic strain does not decrease once it has started.

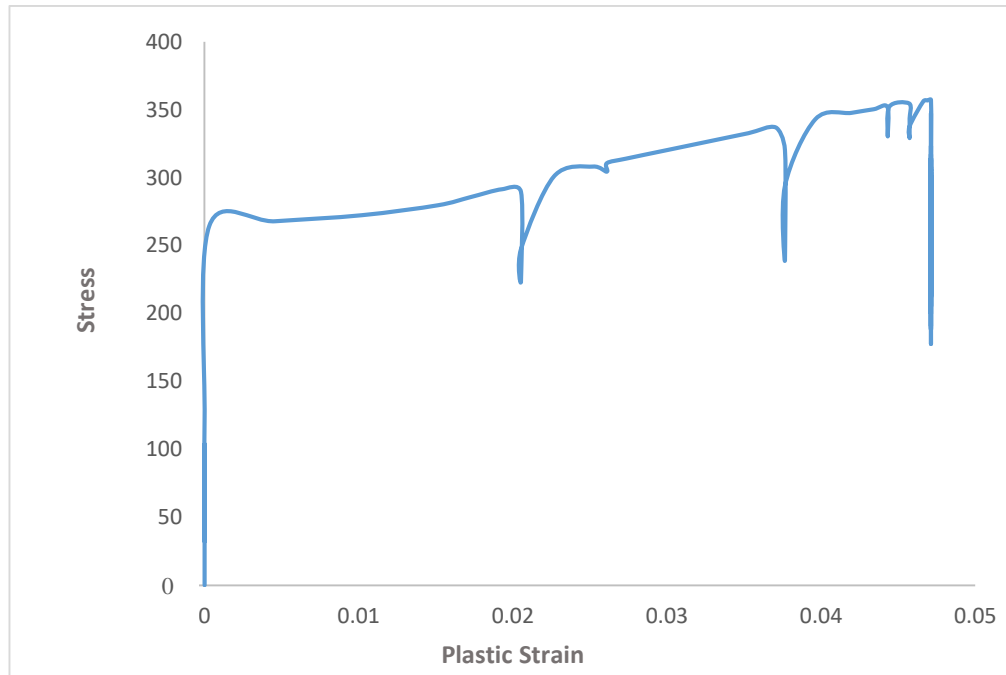


**Figure 4.11.** Stress vs. plastic strain history on element 119.

Ductile damage initiation criterion (DUCTCRT) in the results, denotes the occurrence of damage on an element if its value becomes 1. Its value on member 119 reached only up to 0.483, which is not enough to start stiffness degradation of the material. Even though the damage criterion value increased from 0.141 in the first analysis to 0.483 in the second analysis, still this value is very small than 1 to start the damage process. This much plasticity on the element is not a major risk of concern because no element lost its load-bearing capacity and the stiffness degradation did not occur. Hence, the load transfer mechanism in transmission tower will not get affected.

#### **4.4 Seismic Load on Transmission Tower**

In this section, the investigation of the damages caused in transmission tower members when subjected to strong earthquakes will be focused. As shown previously in chapter 3, all the necessary aspects for running the non-linear dynamic analysis such as the step, amplitude, boundary conditions, loads, and mesh were defined. El Centro ground motion record was selected as an input to investigate the collapse mechanism of transmission tower under seismic loads. While the analysis is going, if any element in structure loses

load-bearing capacity, it gets removed. As the effect of seismic load on the structure continues, more and more elements will lose load-bearing capacity, thus causing the collapse of the tower. The tower was analyzed by setting the analysis duration for 20 seconds while keeping material and geometric nonlinearity active.

The nonlinear seismic response analysis of the lattice transmission tower stopped at 13.50 second due to extreme damage in the members available in the top section of the structure. Figure 4.12 illustrates the collapse mode of a transmission tower and also captures the final moment when the analysis stopped.

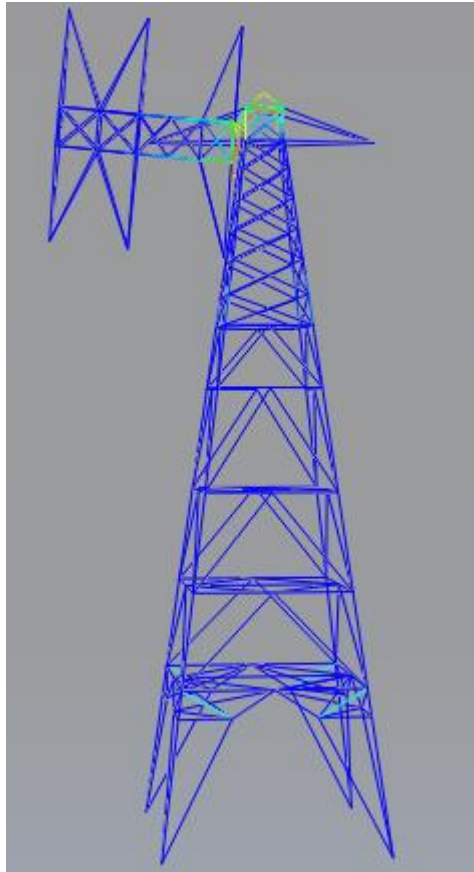


**Figure 4.12.** Collapse mode of transmission tower

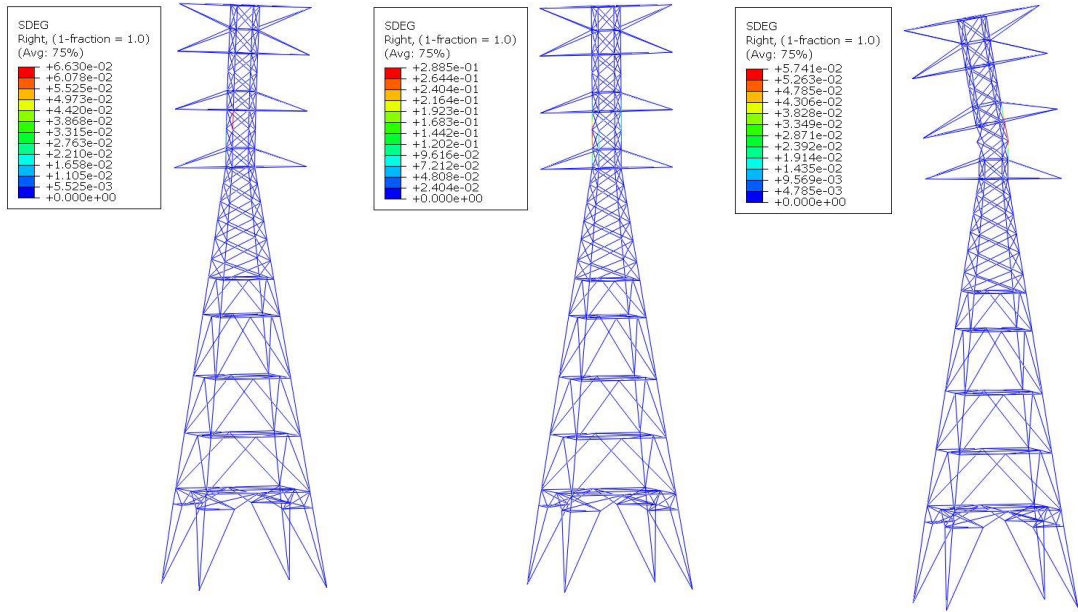
The collapse mechanism and collapse process of the tower are discussed, respectively. Throughout the analysis, plastic strains were recorded in various members of the structure. It can be seen that the top section of tower is extremely deformed due to the

presence of many failed elements distributed in the panel M and panel N. The massive deformation surpasses the normal working limit, which further leads to the tower collapse.

#### **4.4.1 Collapse Process of Transmission Tower**

The collapse details of the transmission tower under the El Centro earthquake excitations are shown in Figure 4.13.

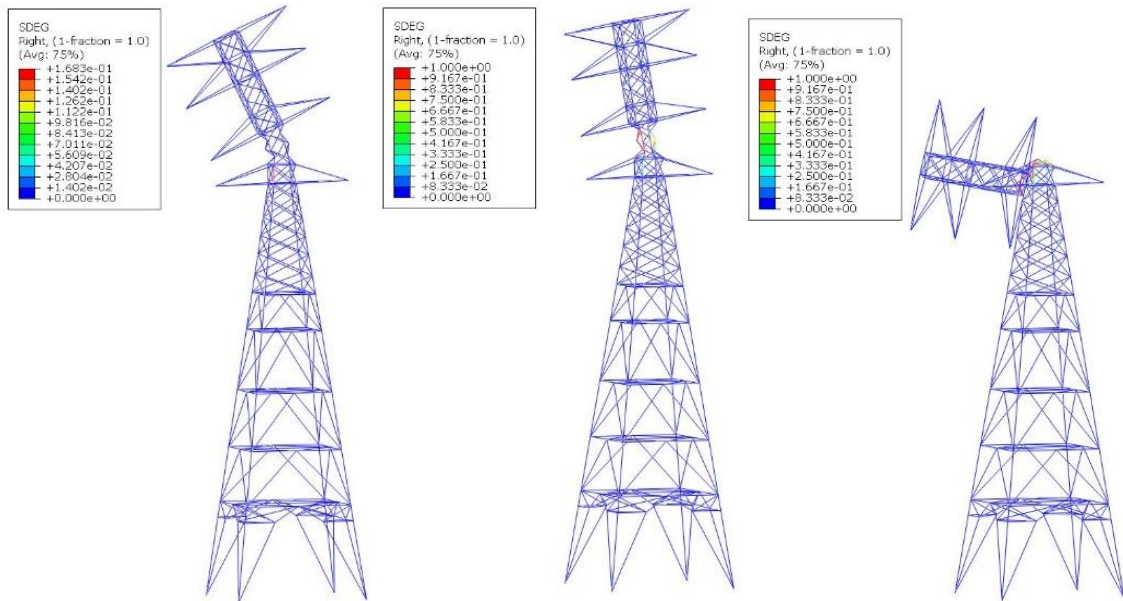
At the initial stage, when  $t = 2.48$  s (Figure 4.13(a)), the damage index  $D$  of vertical leg member 223 in the panel N is equal to 0.066, which indicates that the damage has started on this member. When  $t = 2.64$  s (Figure 4.13(b)), the damage index of the leg member 223 reaches 1, and the member loses bearing capacity. As soon as this member fails, it gets removed from the analysis, and the load transfer mechanism changes its path. Some tower members get extra loaded, whereas some members get unloaded. When  $t = 2.78$  s (Figure 4.13(c)), leg members on the earthquake side of panel M and N get fully damaged and fail, whereas the leg members on the leeward side in panel M and N are still there with less damage occurred. Due to the failure of leg members on the earthquake side of the tower, the leg members on leeward side undergo high stresses, which leads to high plasticity. Subsequently, when  $t = 5.56$  s (Figure 4.13(d)) stiffness degradation all the leg members in panel M and N reaches the maximum capacity and fails completely. This leads to the redistribution of internal forces to the other members of tower. After this point, the top portion of tower is very unstable and is at high risk to collapse anytime because all the lateral forces in panel M and N are resisted by the braces only. When  $t = 9.74$  s (Figure 4.13(e)), most of the braces in panel M and N start getting damaged and its stiffness degradation initiates due to the presence of high stresses and intense plasticity. As the stiffness degradation continues, these diagonal members reach their load-carrying capacity and fail one by one. Failure of these diagonal members makes the top section of tower tilt laterally. Finally, when  $t = 13.50$  s, the top section of tower gets dislocated from its original position. It can be seen that the failure of vertical leg members in panel M and N will trigger the collapse of the tower.



a)  $t = 2.48$  s, damage initiation of a leg member 223 in panel N.

b)  $t = 2.64$  s, element 223 removed after failing completely.

c)  $t = 2.78$  s, some leg members in panel M failed completely.



d)  $t = 5.56$  s, all the leg members in panel M and N failed completely.

e)  $t = 9.74$  s, bracings in panel M and N damaged.

f)  $t = 13.50$  s, collapse of the top portion of tower.

**Figure 4.13.** Collapse details of the lattice transmission tower under earthquake excitations.

#### 4.4.2 Behavior of Element 223

Critical element 223 was the first member of the transmission tower system to fail under seismic loads therefore, it is important to understand the behavior and history of this element. This element is responsible for triggering the collapse of the top portion of the tower. Element 223 is located 43.7 m above from the ground level, serving as a vertical leg member of the transmission tower located in the panel N.

The stress history curve of element 223 is presented in Figure 4.14 below. The element experiences small stresses as soon as the analysis started. Sharp increase in the stress values occurring on the element due to the large seismic loads can be seen clearly from the graph. The stresses kept on increasing until the maximum stress of 415 MPa is reached. Shortly after crossing the maximum stress, the overall stress on the element reduces and drops down to zero at 2.62 seconds. This inability of an element to take more stresses indicates the failure of an element.

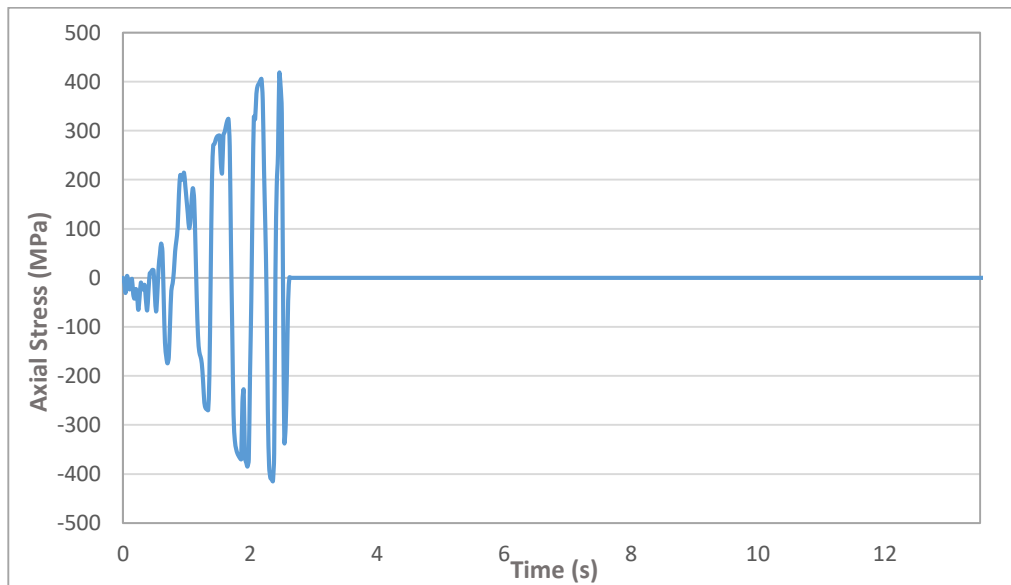


**Figure 4.14.** Stress time history curve of element 223.

The plastic strain time history in element 223 is presented in Figure 4.15. Plastic strain in the element started as soon as the stress component (S11) crossed the yield stress value of 264 MPa after 1.3 seconds. Once the plastic strain on the element started, it kept on

increasing sharply due to the presence of large stress values. The plastic strain finally became constant with no change in its values after 2.62 seconds because of absence of strain.

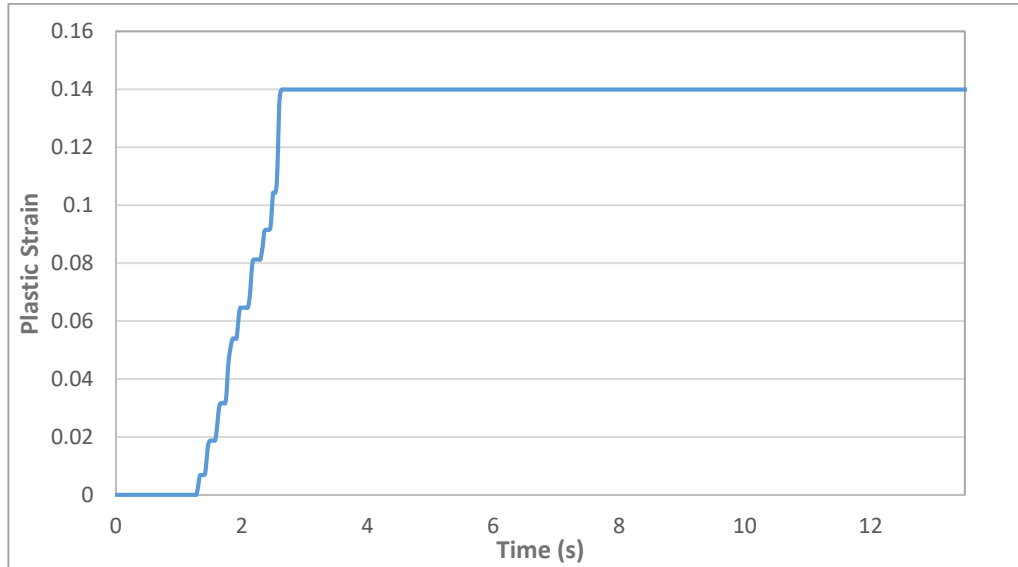


**Figure 4.15.** Plastic strain time history of element.

Stress vs. strain curve for element 223 under cyclic forces is given in Figure 4.16.

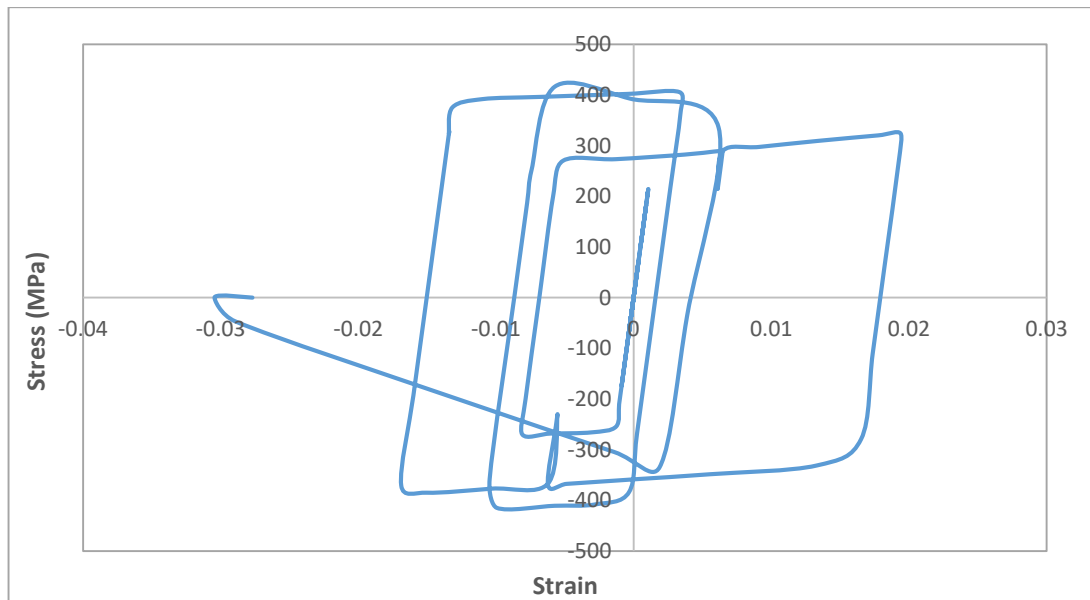


**Figure 4.16.** Stress time history curve of element 223.

The trend in the growth of internal force on the member 223 can be seen increasing rapidly along the time from Figure 4.17. The element reaches its maximum capacity of 160 kN on 2.48 seconds first and then reduces and subsequently becomes zero on 2.64 seconds; this is due to the presence of damage on the member because of which it cannot bear the load anymore.

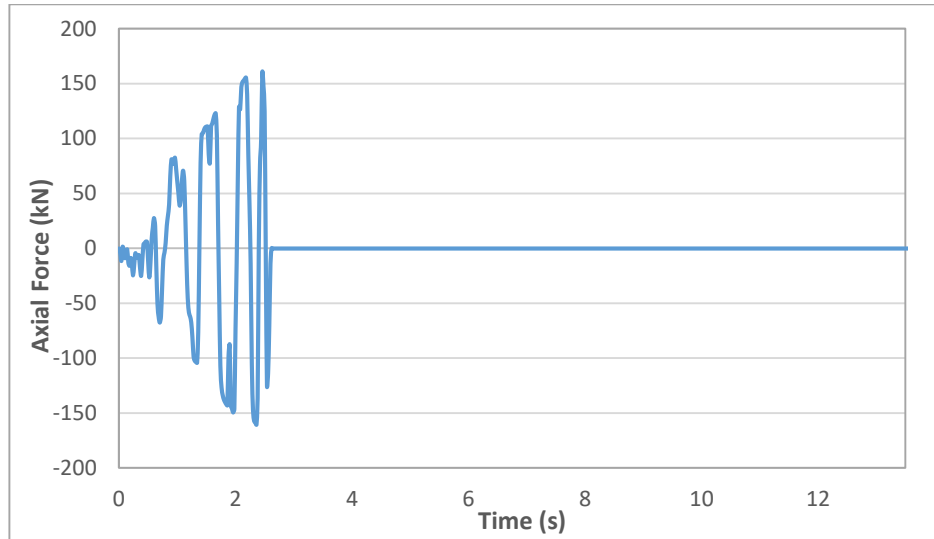


**Figure 4.17.** Axial force-time history curve of element 223.

#### Damage history of element 223

Along with the initiation of plasticity on the member, the ductile damage initiation criterion (DUCTCRT) also came into existence by beginning with a very small value of 0.018, as shown in Figure 4.18. The damage (stiffness degradation) is said to have started if this criterion becomes equal to 1. After crossing the yield stress value, the plastic strain kept on increasing sharply along with the increase in the damage initiation criterion. The damage initiation criterion (DUCTCRT) got satisfied by becoming equal to 1 at 2.48 seconds, indicating the initiation of damage on the member.

Hand calculations to verify the initiation of damage on an element 223 can be done by using Equation 3.5, as mentioned in unit 3 of this thesis.

$$\Delta\omega_D = \frac{\Delta\bar{\epsilon}^{pl}}{\bar{\epsilon}_D^{pl}(\eta, \bar{\epsilon}^{pl})}$$



$$\Delta\omega_D = \frac{0.0978}{0.0948} = 1.03$$

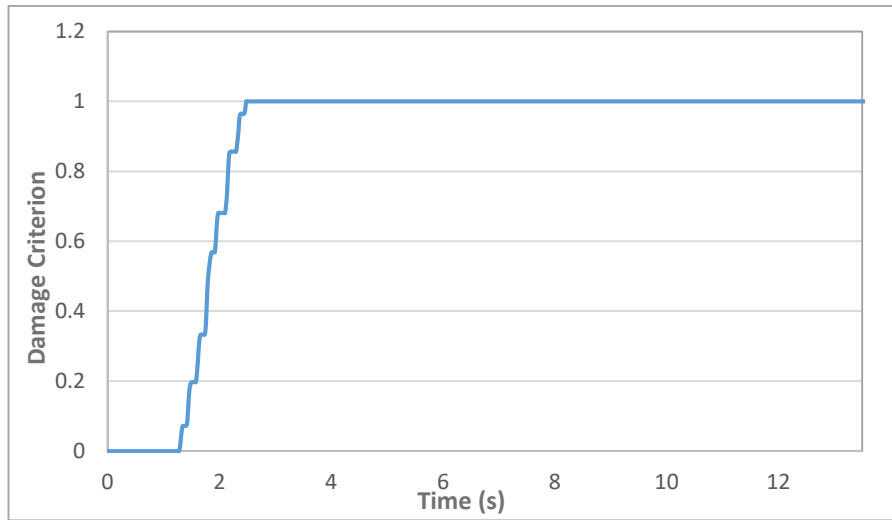


**Figure 4.18.** Ductile damage time history of element.

Since the damage initiation criterion ( $\Delta\omega$ ) has been satisfied (i.e., became equal to 1) at 2.48 seconds, now at the same moment stiffness degradation (damage) of material will also start as shown in figure 4.19.

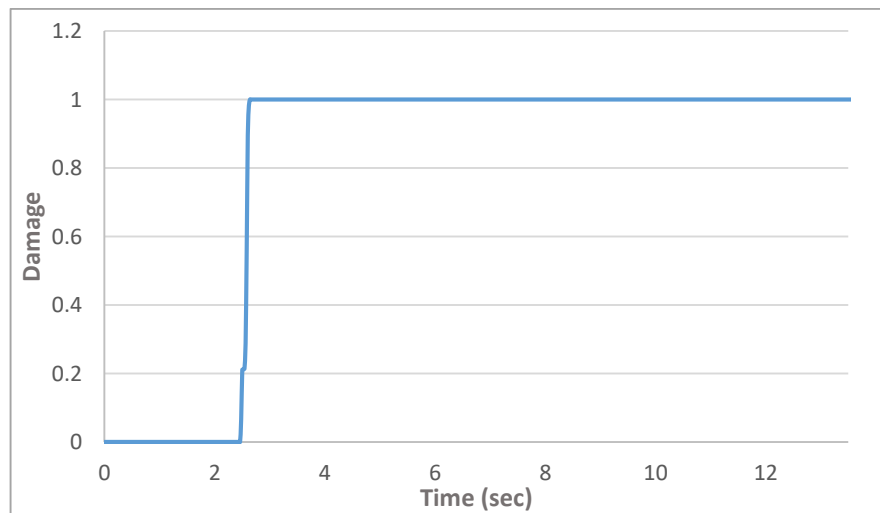


**Figure 4.19.** Damage time history of element

Stiffness degradation of material will continue until the entered parameter for the 'Displacement at failure' is solved by the Abaqus solver. Finally, element 223 gets completely degraded, which is indicated by SDEG showing its value as 1. After the element got completely degraded at 2.64 seconds, it is removed from the analysis, and the load distribution mechanism of the system changes. Other elements in the panel M and N also followed the same trend of failing one by one like element 223. The subsequent failure of leg members, followed by diagonal bracing members' failure, led to the collapse of the top portion of transmission tower.

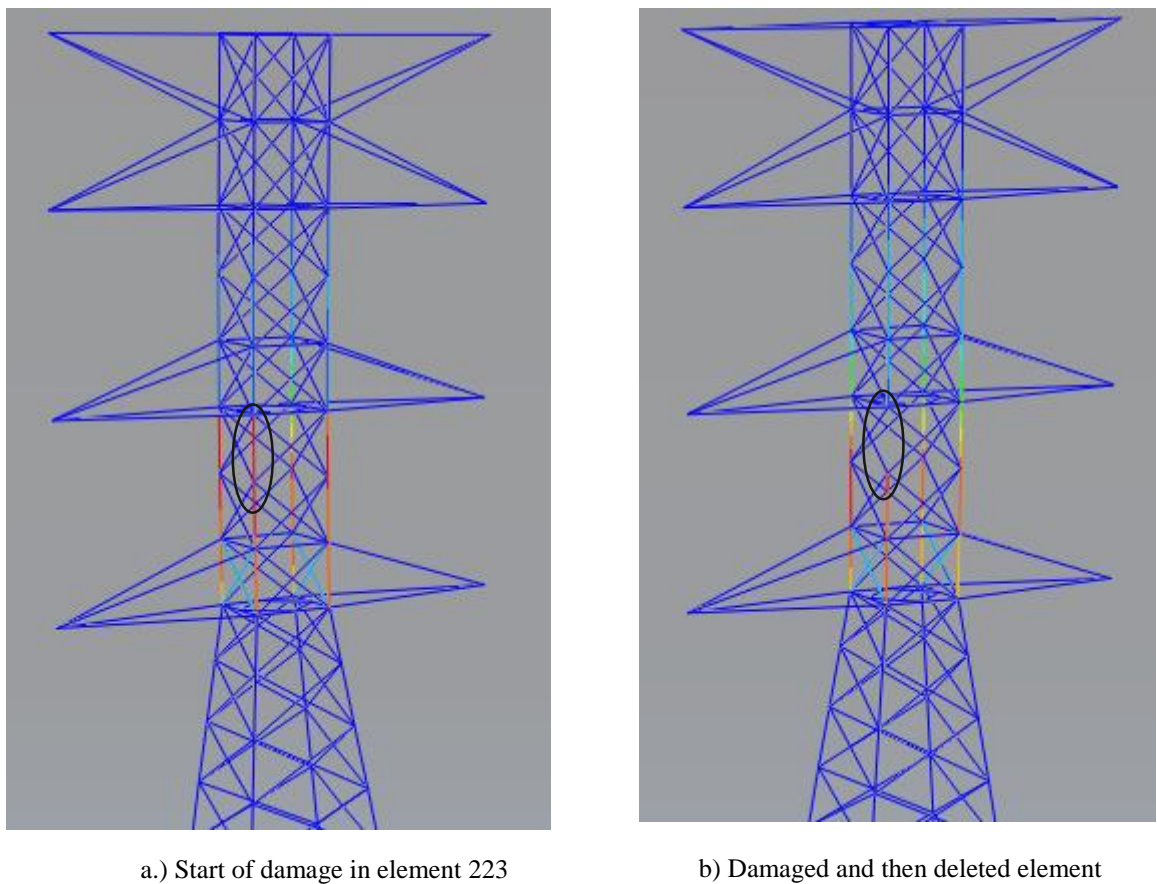


**Figure 4.20.** Damage initiation and failure of element 223

It can be noticed that the collapse pattern occurred in tower model used in this work matches with the collapse pattern occurred in the previous transmission tower failures as shown in figure 1.3 of 1<sup>st</sup> chapter.

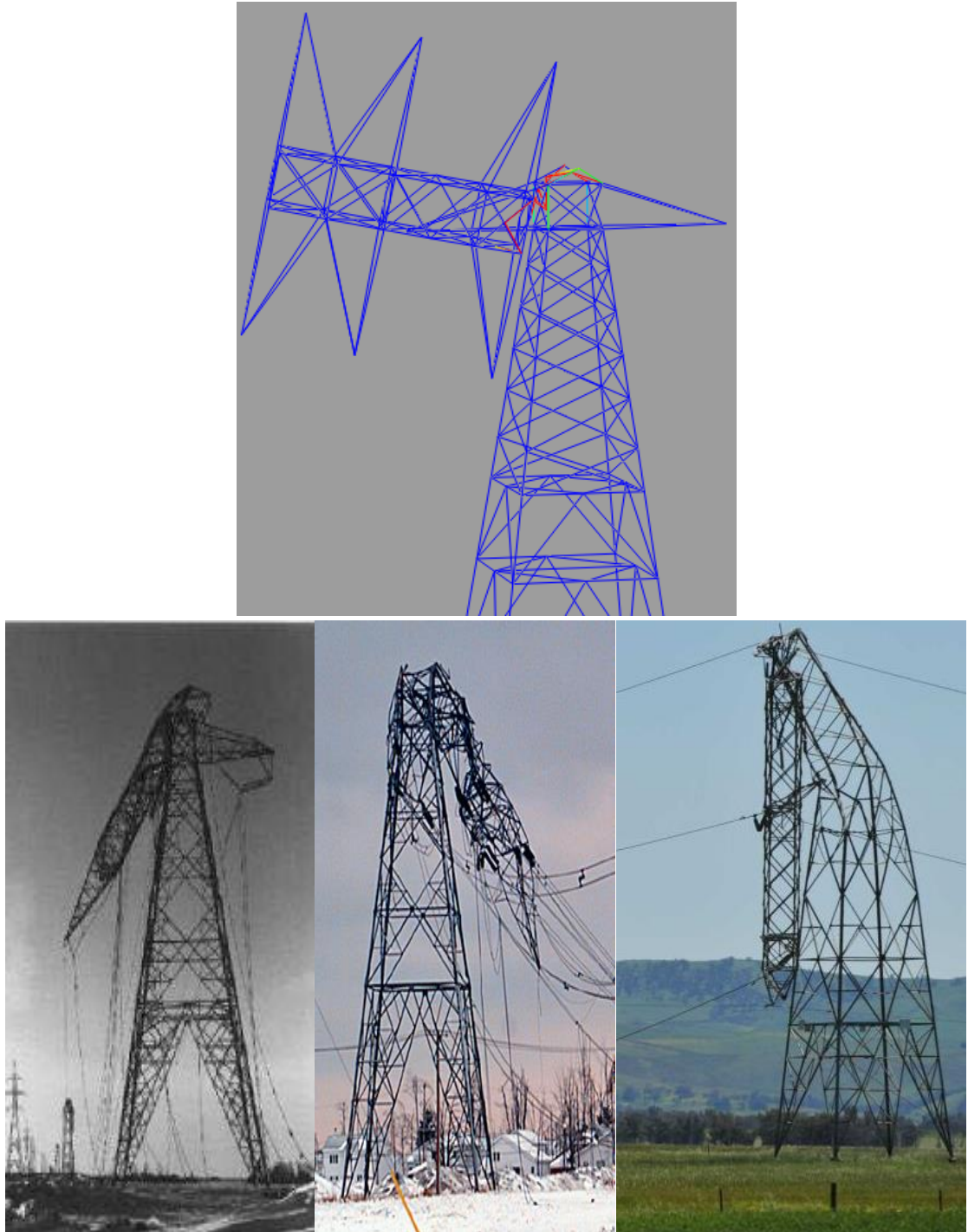


**Figure 4.21.** Similarity between the transmission tower collapse using Abaqus and real-life events.

## 5. CONCLUSION

In this work, the collapse analyses of a lattice transmission tower under wind load and seismic load are carried out. The steel material model was developed and utilized to capture the non-linear behavior of elements in the tower by taking plasticity, damage effect, and ductile failure criterion into consideration. The damage mechanism of elements and collapse mechanism of the structure using time history analysis is discussed. Based on the results achieved from this investigation, the following crucial conclusions are drawn.

1. The steel material model developed in this work is effective in capturing the non-linear behavior of the element, capturing the cumulative damage on the element, and simulate the realistic collapse process of the lattice transmission tower.
2. The damage potential in the vertical leg members of panel M and N is very high. Redistribution of internal forces in the structure caused by the continuous failures of elements in these panels results in the collapse of the tower. Therefore, more attention should be paid to the seismic design of these members.
3. The progressive collapse simulation can be a very effective method to predict the weak position of the lattice tower. In this work, panel M and N were determined to be weak areas of the tower.
4. The failure of element 223 is responsible for triggering the progressive collapse of the tower subjected to El Centro ground motion. This element is more susceptible to damage than other elements in the tower.
5. The tower survived the largest wind loads with minimum damage in a few leg members at panel M. Therefore, wind loads were not the major cause of concern in this work.
6. The procedure suggested in this work is efficient, so this procedure can be applied for designing a new lattice tower, for controlling the capacity of an existing tower or for reinforcement of current structures.

Due to the complex structure of the lattice transmission tower, it is tough to give a general conclusion from the investigation of a single structural model. Nevertheless, this work

demonstrates the method of how the progressive collapse in the transmission tower can be developed and how its failure can be investigated. Moreover, the result from this work shows the significance of considering the damage parameters on the seismic response of tower. More researches are required further to profoundly investigate the effects and responses of the tower under different circumstances.

## REFERENCES

- American Society of Civil Engineer, A. 2013.** Minimum design loads for buildings and other structures. Virginia, Published by *American Society of Civil Engineers*.
- An, L., Wu, J., Zhang, Z., Zhang, R. 2018.** Failure analysis of a lattice transmission tower collapse due to the super typhoon Rammasun in July 2014 in Hainan Province, China. Published by *Journal of Wind Engineering and Industrial Aerodynamics*, 182, 295-307.
- Ahmed, K. I. 2007.** Finite element modeling of non-linear structural response of transmission towers including bolted joint slippage, Published by *University of British Columbia*.
- Abaqus, V. 2014.** 6.14 Documentation/User Manual, Dassault Systemes Simulia Corporation, <http://ivt-abaqusdoc.ivt.ntnu.no:2080/texis/search/?query=wetting&submit.x=0&submit.y=0&group=bk&CDB=v6.14>
- China Architecture & Building Press 2006.** Code for Design of High-Rising Structures, GB50135-2006, Beijing, China.
- Cormie, D. 2013.** Manual for the Systematic Risk Assessment of High-risk Structures Against Disproportionate Collapse, October 2013. Published by *Institution of Structural Engineers*.
- Cuoco, D. A. 1997.** Guidelines for the Design of Double-Layer Grids. American Society of Civil Engineers. Available from: <https://cedb.asce.org/CEDBsearch/record.jsp?dockey=0108492>
- Eslamlou, S. D., Asgarian, B. 2017.** Determining critical areas of transmission towers due to sudden removal of members. Published by *Case studies in engineering failure analysis*, 9, 138-147.
- Eltaly, B., Saka, A., & Kandil, K. 2014.** FE simulation of transmission tower. *Advances in Civil Engineering*
- Faulkner, D. 2016.** South australia storm damage. Online available at <https://www.abc.net.au/news/2016-10-01/damaged-transmission-tower-near-melrose-south-australia-storms/7895742?nw=0>
- Fu, X., Wang, J., Li, H. N., Li, J. X., & Yang, L. D. 2019.** Full-scale test and its numerical simulation of a transmission tower under extreme wind loads. *Journal of Wind Engineering and Industrial Aerodynamics*, 190, 119-133.
- Gooseman, 2020.** <https://www.cgtrader.com/3d-models/exterior/industrial/electric-transmission-towers>

**Hamada, A., El Damatty, A. A., Hangan, H., Shehata, A. Y. 2010.** Finite element modelling of transmission line structures under tornado wind loading. *Wind and Structures*, 13(5), 451.

**Jiang, W. Q., Wang, Z. Q., McClure, G., Wang, G. L., Geng, J. D. 2011.** Accurate modeling of joint effects in lattice transmission towers. *Engineering Structures*, 33(5), 1817-1827.

**Loh, C. H., Tsay, C. Y. 2001.** Responses of the earthquake engineering research community to the Chi-Chi (Taiwan) earthquake. Published by *Earthquake Spectra* 17(4): 635-656.

**Pavlović, M., Marković, Z., Veljković, M., & Buđevac, D. 2013.** Bolted shear connectors vs. headed studs behaviour in push-out tests. *Journal of Constructional Steel Research*, 88, 134-149.

**Rao, N. P., Kalyanaraman, Venkatakrisnan. 2001.** Non-linear behaviour of lattice panel of angle towers. Published by *Journal of Constructional Steel Research*, 57(12), 1337-1357.

**Rao, N. P., Knight, G. S., Lakshmanan, N., Iyer, N. R. 2010.** Investigation of transmission line tower failures. Published by *Engineering Failure Analysis*, 17(5), 1127-1141.

**Siddam, A. 2014.** Cascade failure analysis of electrical transmission lines using ADINA. Published by *Memorial University of Newfoundland*. Online available at <https://research.library.mun.ca/6273/>

**Shehata, A. 2020.** Cascade Failure of Transmission Lines under Downbursts. Published by *The University of Western Ontario*.

**Tian, L., Ma, R., Wang, W., Wang, L. 2013.** Progressive Collapse Analysis of Power Transmission Tower Under Earthquake Excitation, *The Open Civil Engineering Journal*, 2013, 7(1): 164-169.

**Tian, L., Pan, H., Ma, R., Zhang, L., Liu, Z. 2019.** Full-scale test and numerical failure analysis of a latticed steel tubular transmission tower. Published by *Engineering Structures*, 109919.

**Tian, L., Guo, L., Ma, R., Gai, X., Wang, W. 2018.** Full-scale tests and numerical simulations of failure mechanism of power transmission towers. *International Journal of Structural Stability and Dynamics*, 18(09), 1850109.

**Tian, L., Gai, X. 2016.** Non-linear seismic behavior of different boundary conditions of transmission line systems under earthquake loading. Published by *Shock and Vibration*, 2016.

**Wikipedia 2019.** Progressive Collapse. Online available at: [https://en.wikipedia.org/wiki/Progressive\\_collapse](https://en.wikipedia.org/wiki/Progressive_collapse)

**Wurst, B. 2017.** Will climate change effect our winter? Online available at: <https://miltimes.ca/Montreal/social-life/montreal-times-environment-information/will-climate-change-effect-our-winter/>

**Wang, W. M., Li, H. N., Tian, L. 2013.** Progressive collapse analysis of transmission tower-line system under earthquake. Published by *Advanced Steel Construction*, 9(2): 161-172.

**Zhang, Z., Li, H., Li, G., Wang, W., Tian, L. 2013.** The numerical analysis of transmission tower-line system wind-induced collapsed performance. *Mathematical Problems in Engineering*. <https://www.hindawi.com/journals/mpe/2013/413275/>



## **RESUME**

Name Surname : Aiman Tariq  
Place and Date of Birth : Kashmir, 15 December 1994  
Foreign Languages : Turkish, Hindi, Kashmiri

Education Status  
High School : Army Public School, Srinagar/Kashmir (2013)  
Bachelor's : Punjab Technical University, Punjab/India (2017)  
Master's : Bursa Uludag University, Bursa/Turkey (2020)

Work Experience : J&K Roads and Buildings Construction Dept.,  
Srinagar/Kashmir (4 months), 2017

Contact (e-mail) : aimantariq1@gmail.com